The Partial Elements Equivalent Circuit Method: The State of the Art

Giulio Antonini ®, *Senior Member, IEEE*, Albert E. Ruehli, *Life Fellow, IEEE*, Daniele Romano ®, and Fabrizio Loreto ®

Abstract—**This year marks about half a century since the birth of the technique known as the partial element equivalent circuit modeling approach. This method was initially conceived to model the behavior of interconnect-type problems for computer-integrated circuits. An important industrial requirement was the computation of general inductances in integrated circuits and packages. Since then, the advances in methods and applications made it suitable for modeling a large class of electromagnetic problems, especially in the electromagnetic compatibility (EMC)/signal and power integrity (SI/PI) areas. The purpose of this article is to present an overview of all aspects of the method, from its beginning to the present day, with special attention to the developments that have made it suitable for EMC/SI/PI problems.**

Index Terms—**Circuit modeling, electromagnetic modeling, Kirchhoff laws, Maxwell's equations, partial element equivalent circuit (PEEC) method.**

I. INTRODUCTION

THE numerical solutions of Maxwell's equations were significantly enhanced between the end of the '60s to the '70s. Until then, Maxwell's equations were used to obtain analytical solutions. The numerical solutions were rapidly advanced with the first more powerful computers. Then, within a few years, we witnessed the birth of several fundamental numerical approaches which are in use today. Among them, we list the finite difference time domain (FDTD) method [1], the finite element method (FEM) [2], the method of moments (MoM) [3], [4], and the finite integration technique (FIT) [5].

The partial element equivalent circuit (PEEC) method also was conceived in the early '70s. The IBM mainframe computers which were the most advanced at that time, required modeling with more complicated inductive interconnect topologies. Specifically, the electronic system problem required relatively complex numerical modeling of inductive voltage drop in the

power and ground voltages connected to ICs. The concept of partial inductance-based complex circuit analysis was introduced in [6], where it was shown how to solve circuits based on multiple parts of conductors of finite length. This made complex inductive structure models solvable.

Integrated circuit design and packaging also required the calculation with capacitive elements. The capacitance computation for 3-D conductors was presented in [7] using the concept of co-efficient of potential. The two concepts of partial inductance and coefficient of potential were integrated into the integral equation-based formulation published in [8], which can be considered the foundation of the PEEC method. More than 20 years after the introduction of PEEC, the applications were mostly in the modeling of interconnections in printed circuit boards [9], [10] and packaged electronics [11], including dielectric as well [12], [13].

New applications of PEEC, other than that of interconnections date back to 1998. Specifically, new problems like the modeling of lightning protection systems and its coupling to coaxial cables were solved [14].

Since then, there has been a growing interest in the PEEC method which has been applied to a large variety of different fields including power electronics [15], [16], [17], [18], [19], [20], power systems [21], [22], antennas [23], [24], [25], [26], [27], [28], [29], [30], radio-frequency integrated circuits (RFICs) [31], [32] and RF interferences [33], lightning [34], [35], [36], filters [37], [38], on-chip interconnects [39], frequency selective surfaces [40], [41], [42], Litz wires [43], [44], [45], [46], neuromorphic chip crossbar array [47], flexible electronics [48], [49], high-temperature superconducting (HTS) cables [50], decoupling capacitors [51], wireless power transfer [52], [53], [54], and return network in composoite aircraft [55], just to name a few. The list of applications and contributors increases continuously due to recent improvements. Furthermore, up to date, two books [56], [57] have been published on the PEEC method. Other books have chapters or sections devoted to PEEC [58],[59, Ch.6], [60].

The number of papers on the PEEC method has been constantly increasing over the years, as shown in Fig. 1.

An important added value of the PEEC method is represented by the fact that, by providing a circuit interpretation of Maxwell's equations, it is totally compatible with circuit solvers, such as SPICE [61], [62], [63]. A SPICE solver modified to take the propagation into account has been presented in [64].
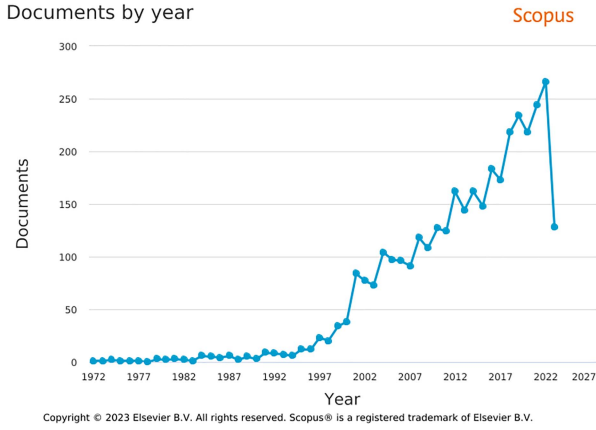
Fig. 1.   Number of articles on the PEEC method from 1972 to present.

It is also worth mentioning that the PEEC method is listed among the numerical methods to solve Maxwell's equations listed in the IEEE Standard for Validation of Computational Electromagnetics Computer Modeling and Simulations (IEEE Std 1597.1-2008) [65].

In this work, we retrace the 50 years' history of the method and the evolution that led it to be considered today among the most suitable ones to be used in the field of electromagnetic compatibility (EMC), signal, and power integrity (SI/PI).

II. BASIC PEEC FORMULATION

The PEEC method is based on the electric field integral equation (EFIE) and the continuity equation (CE). Differently from the MoM (Z-MoM) [3], the continuity equation is kept separate from the EFIE such that the solution includes both currents as well as potentials or charges. The basic derivation of PEEC equations is carried out in this section for a conductor in the Laplace domain. The modeling of different materials is described in Section V.

The electric field at a point $\mathbf{r}$ in a conductor is

$$\mathbf{E}(\mathbf{r},s) = \frac{\mathbf{J}(\mathbf{r},s)}{\sigma} = \mathbf{E}^{\text{inc}}(\mathbf{r},s) - s\mathbf{A}(\mathbf{r},s) - \nabla\Phi(\mathbf{r},s) \quad (1)$$

where σ is the conductor conductivity, $\mathbf{E}^{\text{inc}}(\mathbf{r},s)$ is the external electric field impressed at point $\mathbf{r}$ at a Laplace frequency s. $\mathbf{A}(\mathbf{r},s)$ and $\Phi(\mathbf{r},s)$ are the magnetic vector and electric scalar potentials [66], respectively. They read

$$\mathbf{A}(\mathbf{r},s) = \frac{\mu_0}{4\pi}\int_{V'}\frac{\mathbf{J}(\mathbf{r}',s)e^{-s\tau}}{|\mathbf{r}-\mathbf{r}'|}dV' \quad (2)$$

and

$$\Phi(\mathbf{r},s) = \frac{1}{4\pi\varepsilon_0}\int_{V'}\frac{q(\mathbf{r}',s)e^{-s\tau}}{|\mathbf{r}-\mathbf{r}'|}dV' \quad (3)$$

where $\tau = |\mathbf{r}-\mathbf{r}'|/c_0$ is the speed of light in the background medium. If we replace the vector potential $\mathbf{A}(\mathbf{r},s)$ in (1), we get

$$\mathbf{E}^{\text{inc}}(\mathbf{r},s) = \frac{\mathbf{J}(\mathbf{r},s)}{\sigma} + s\frac{\mu_0}{4\pi}\int_{V'}\frac{\mathbf{J}(\mathbf{r}',s)e^{-s\tau}}{|\mathbf{r}-\mathbf{r}'|}dV' + \nabla\Phi(\mathbf{r},s) \quad (4)$$

which has $\mathbf{J}(\mathbf{r},s)$ and $\Phi(\mathbf{r},s)$ to be determined. In addition to the EFIE, the continuity equation is used

$$\nabla\cdot\mathbf{J}(\mathbf{r},s) = -sq(\mathbf{r},s) \quad (5)$$

that makes the problem well-posed. If the charges are assumed to be located on the surface of volumes, which is a reasonable hypothesis for good conductors, then the continuity equation has to be written as

$$\nabla\cdot\mathbf{J}(\mathbf{r},s) = 0 \qquad \mathbf{r}\in V' \quad (6a)$$

$$\nabla\cdot\mathbf{J}(\mathbf{r},s) = -sq_s(\mathbf{r},s) \quad \mathbf{r}\in S'. \quad (6b)$$

In this case, the electric scalar potential has to be redefined as

$$\Phi(\mathbf{r},s) = \frac{1}{4\pi\varepsilon_0}\int_{S'}\frac{q_s(\mathbf{r}',s)e^{-s\tau}}{|\mathbf{r}-\mathbf{r}'|}dS'. \quad (7)$$

Then, current and charge densities $\mathbf{J}(\mathbf{r},s)$ and $q(\mathbf{r},s)$ are expanded in terms of pertinent basis functions $\mathbf{b}\in\mathcal{R}^3$ and $p\in\mathcal{R}$

$$\mathbf{J}(\mathbf{r},s) \cong \sum_{n=1}^{N_v}\mathbf{b}_n(\mathbf{r})I_n(s) \quad (8a)$$

$$q(\mathbf{r},s) \cong \sum_{j=1}^{N_s}p_j(\mathbf{r})Q_j(s) \quad (8b)$$

where $I_n(s)$ and $Q_j(s)$ are the expansion weights that must be determined at each angular frequency s, N_v and N_s represent the number of the elementary volume and surface regions, respectively. Then, expansions (8) are substituted into (2)–(4), and (6) and the so-called Galerkin's testing or weighting process [67] is used to generate a system of equations for the unknowns weights $I_n(s), n = 1,\ldots,N_v$ and $Q_m(s), m = 1,\ldots,N_s$ by enforcing the residuals of (3)–(5) to be orthogonal to a set of weighting functions that are chosen coincidently with the basis functions. Then, two inner products are defined

$$\langle\mathbf{b}_m(\mathbf{r}),\mathbf{f}(\mathbf{r})\rangle = \int_{V_m}\mathbf{b}_m(\mathbf{r})\cdot\mathbf{f}(\mathbf{r})\,dV_m \quad m = 1,\ldots,N_v \quad (9a)$$

$$\langle p_j(\mathbf{r}),g(\mathbf{r})\rangle = \int_{S_i}p_j(\mathbf{r})g(\mathbf{r})\,dS_j \quad i = 1,\ldots,N_s. \quad (9b)$$

They are used to average (4) and (6) on elementary volumes and (7) on elementary surfaces. Importantly, the averaging process leads to double integration in the partial elements, e.g., (21) and (28), making symmetric the corresponding matrices.

The Galerkin's method applied to the EFIE (4) yields, in a matrix form

$$-\mathbf{A}^T\mathbf{\Phi}(s) + \mathbf{R}\mathbf{I}(s) + s\mathbf{L}_p(s)\mathbf{I}(s) = \mathbf{V}_s(s) \quad (10)$$

where vectors $\mathbf{\Phi}(s)$ and $\mathbf{I}$ collect the potentials to infinity and the currents flowing through the volumes, respectively, the matrix $\mathbf{A}$ is the usual circuit incidence matrix, $\mathbf{R}$ is a matrix accounting for conductor losses, $\mathbf{L}_p$ is the partial inductance matrix that models the magnetic field/inductive coupling due to the currents, and vector $\mathbf{V}_s(s)$ represents the voltages induced on elementary volumes by the incident electric field $\mathbf{E}^{\text{inc}}(\mathbf{r},s)$ [68].
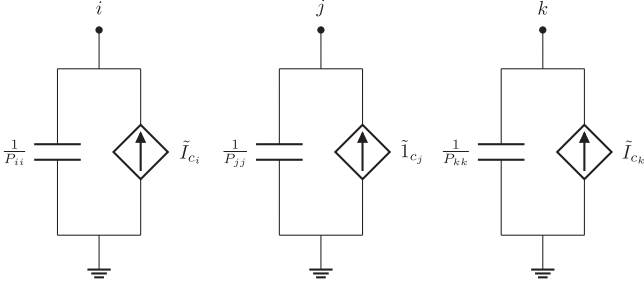
Fig. 2. Equivalent circuit modeling the displacement currents in the background medium.

Equation (10) can be regarded as the Kirchhoff voltage law (KVL) enforced to loops constituted by each ohmic-inductive branch and its closures at infinity.

Applying the Galerkin's method to (6) and (7) yields

$$s\mathbf{Q}(s) + \mathbf{Y}(s)\mathbf{\Phi}(s) + \mathbf{A}\mathbf{I}(s) = \mathbf{I}_s(s) \tag{11}$$

and

$$\mathbf{\Phi}(s) = \mathbf{P}(s)\mathbf{Q}(s) \tag{12}$$

where matrix $\mathbf{Y}(s)$ models lumped elements and vector $\mathbf{I}_s(s)$ accounts for eventual lumped current sources.

Equation (12) is well suited to identify an equivalent circuit for the displacement currents in the background medium. Indeed, they read

$$\mathbf{I}_c = s\mathbf{Q}(s). \tag{13}$$

Some simple algebraic manipulations allows to rewrite (12) as

$$\mathbf{I}_c = s\mathbf{Q}(s) = s\mathbf{D}\mathbf{\Phi}(s) - \tilde{\mathbf{I}}_c \tag{14}$$

where $\tilde{\mathbf{I}}_c = \mathbf{T}\mathbf{I}_c$ and matrices $\mathbf{D}$ and $\mathbf{T}$ are

$$\mathbf{D} = \begin{bmatrix} \frac{1}{P_{11}} & 0 & \cdots & 0 \\ 0 & \frac{1}{P_{22}} & \cdots & 0 \\ \vdots & \vdots & \vdots & \vdots \\ 0 & 0 & \cdots & \frac{1}{P_{N_s N_s}} \end{bmatrix} \tag{15a}$$

$$\mathbf{T} = \begin{bmatrix} 0 & \frac{P_{12}}{P_{11}} & \cdots & \frac{P_{1N_s}}{P_{11}} \\ \frac{P_{21}}{P_{22}} & 0 & \cdots & \frac{P_{2N_s}}{P_{22}} \\ \vdots & \vdots & \vdots & \vdots \\ \frac{P_{N_s 1}}{P_{N_s N_s}} & \frac{P_{N_s 2}}{P_{N_s N_s}} & \cdots & 0 \end{bmatrix}. \tag{15b}$$

N_s denotes the number of elementary surfaces where the charge is localized. Equation (14) admits the circuit synthesis sketched in Fig. 2 for the case of $N_s = 3$ patches.

Using (12) to eliminate the charges from (11) yields

$$\left[s\mathbf{P}^{-1}(s) + \mathbf{Y}(s) \right] \mathbf{\Phi}(s) + \mathbf{A}\mathbf{I}(s) = \mathbf{I}_s(s). \tag{16}$$

Equation (16) can be regarded as the Kirchhoff current law (KCL) enforced to each node corresponding to elementary

volumes

$$\underbrace{\begin{bmatrix} \mathbf{Y} + s\mathbf{P}^{-1}(s) & \mathbf{A} \\ \mathbf{A}^T & -[\mathbf{R} + s\mathbf{L}_p(s)] \end{bmatrix}}_{\mathbf{N}(s)} \cdot \underbrace{\begin{bmatrix} \mathbf{\Phi}(s) \\ \mathbf{I}(s) \end{bmatrix}}_{\mathbf{X}(s)} = \underbrace{\begin{bmatrix} \mathbf{I}_s \\ -\mathbf{V}_s \end{bmatrix}}_{\mathbf{U}(s)}. \tag{17}$$

Equation (17) is the modified nodal formulation (MNA) of the PEEC circuit [69] equations. It is also worth noticing that additional lumped elements can be easily added to the model just by stamping them into the MNA matrix [57]. We note that the inversion of matrix $\mathbf{P}(s)$ in (17) can be time-consuming when the problem size is large. However, this matrix inversion can be avoided. As an example, the admittance part can be premultiplied by $\mathbf{P}(s)$.

III. MESH GENERATION AND BASIS FUNCTIONS

The choice of the basis functions is directly related to the mesh. Over the years, several different meshing techniques have been considered.

A. Orthogonal Meshing

Initially, the meshing for most PEEC solvers was based on orthogonal Manhattan meshing only, and piecewise constant basis functions were used exclusively [8].

Hence, the basis function for the current density is chosen as

$$\mathbf{b}_n(\mathbf{r}) = \begin{cases} \hat{\mathbf{t}}_n / A_n & \text{if } \mathbf{r} \in V_n \\ \mathbf{0} & \text{otherwise} \end{cases} \tag{18}$$

where $\hat{\mathbf{t}}_n$ is the tangential unit vector for the current direction in volume cell V_n. With such a choice of the basis function, the corresponding weight represents the current flowing in the volume V_n with orientation $\hat{\mathbf{t}}_n$.

Assuming that the free and bound charge densities are located on the surface of conductors, the basis functions used to expand the charge densities are chosen as follows:

$$p_m(\mathbf{r}) = \begin{cases} 1/S_m & \text{if } \mathbf{r} \in S_m \\ 0 & \text{otherwise.} \end{cases} \tag{19}$$

This choice implies that the corresponding weight Q_m represents the charge on cell m and is assumed to be uniformly distributed on the surface.

Fig. 3 shows a simple PEEC ohmic-inductive cell structure for a metal sheet. It represents the layout of the nodes with resistive and inductive cells. Please note that in this example, half-width cells are used at the edge of the conductors so that the cell nodes can be connected at the edge, by assembling the substructures which may consist of multiple sheets. We notice that the inductive and resistive cells are rectangular of zero or a finite thickness. An example of uniform mesh for a finite thickness cell is shown in Fig. 4.

Today, for most problems, the high-frequency skin effect can be included in the model by subdividing the cross-section such that the redistribution of the high-frequency current to the surface can be modeled.
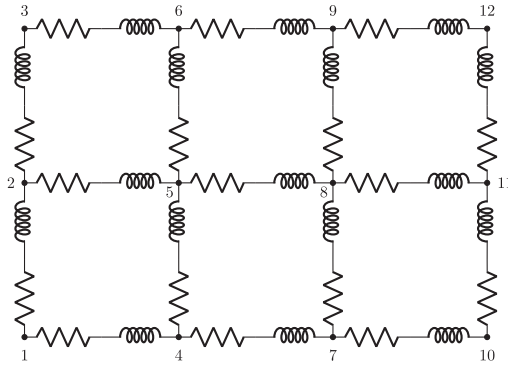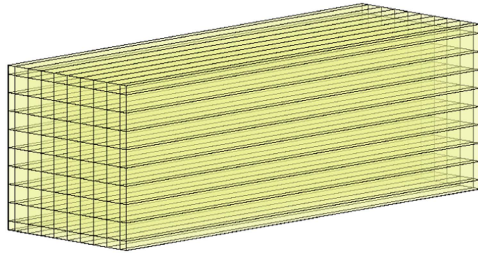
Fig. 3. PEEC circuit of a thin conductive panel.

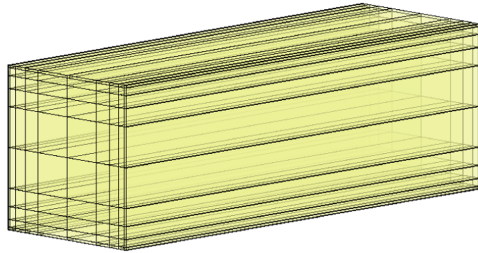
Fig. 4. Volumetric uniform mesh for a simple structure.

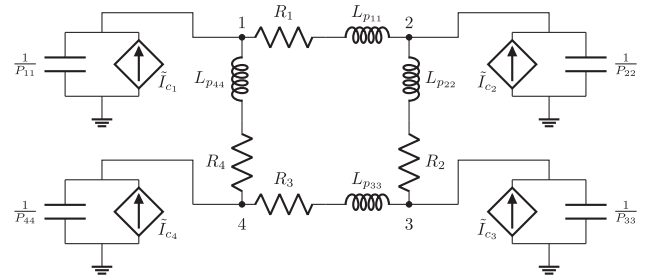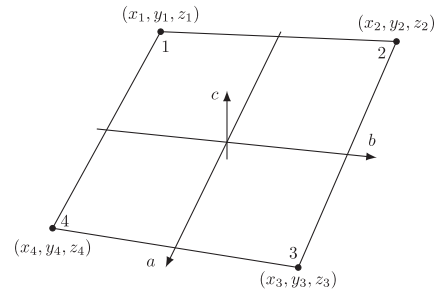Fig. 5. Volumetric nonuniform meshing for a simple structure.

Fig. 6. Example of quadrilateral cell structure.

for the nonuniform distribution of the current density [74], [75]. More recently, it has been coupled to voxellized fast Fourier transform (FFT)-based PEEC models [19].

Finally, skin- and proximity effects can also be efficiently modeled by adopting *ad-hoc* global basis functions, as is done in [76], [77], [78], [79], [80], and [81].

B. Nonorthogonal Meshing

The need to model more complex geometries has led to the development of the PEEC method which is also able to handle problems with non-Manhattan geometry.

Quadrilateral and hexahedral type meshing for PEEC modeling has been developed and presented in [70], [82], [83], [84], and [57, Ch. 7]. An example of a zero-thickness hexahedral cell is given in Fig. 6.

An unstructured PEEC formulation by dual discretization for 2-D geometries has been proposed in [85] and [86] and then used in [87] to analyze two-port TEM cells for VHF applications. Then, it has been extended to volume, dielectric, and magnetic media [88], [89], [90], [91]. A 3-D PEEC formulation for structured and unstructured PEEC models that is based on the cell method [92] has been presented in [93]. It guarantees a circuit interpretation of Maxwell's equations also in magnetic materials and a reduction in the number of degrees of freedom (DoFs) (i.e., required memory) compared to the full-wave unstructured PEEC formulation previously proposed in [89] for electric and magnetic media.

Triangular cells have been applied for a long time in the MoM approach using the Rao–Wilton–Glisson (RWG) basis functions [94], [95]. Triangular meshing has also been considered for the PEEC modeling of conductors in [74], [75], [96], [97], and [98]. Triangular cells have been applied for a long time in the MoM approach using RWG basis functions [94], [95]. Triangular

Thus, when skin-effect has to be caught at high frequencies, the standard PEEC formulation requires a fine mesh of the volume. Such a model can be very inefficient if uniform subsections for the current flow are used, as shown in Fig. 4. However, several different solutions can be used like highly nonuniform meshing [70]. Fig. 5 shows an example of a nonuniform meshing of the cross-section of a conductor.

Theoretically, a surface integral formulation of the PEEC method (e.g., the PMCHWT method) can give a rigorous evaluation of the skin-effect losses for piecewise homogeneous conductors [71], [72]. However, problems may occur in the numerical implementation due to the high contrast between the conductor and the surrounding dielectric, which makes the resultant linear system highly unbalanced. In [73], the interaction integrals involving the curl of the magnetic and electric vector potentials are computed through the Taylor series expansion of the full-wave Green's function, leading to analytical forms that are rigorously derived, thus reducing the numerical issues. When the skin-effect is well-developed, a valuable alternative option is represented by the use of the surface impedance accounting

meshing has also been considered for the PEEC modeling of conductors in [74], [75], [96], [97], and [98].

More recently, an isogeometric analysis (IgA) is proposed for the PEEC method for electrostatic problems in [99]. It is shown that using the spline-based geometry concepts from IgA allows for extracting circuit elements without an explicit meshing step, with a lower number of DoFs and faster convergence compared to the standard PEEC approach.

IV. COMPUTATION OF THE PARTIAL ELEMENTS

Once this decomposition takes place analyzing a given EM problem, it is straightforward to place these effects in a circuit context where electric and magnetic phenomena are always concentrated and well separated, and where each single EM interaction is described by a "partial element." Therefore, the so-called partial elements are subdivided into two categories.

1) *Partial Inductances:* Describing the mutual or self effects due to electric currents flowing through volumes.
2) *Coefficients of Potential:* Describing the mutual or self effects due to electric charges localized on surfaces.
3) Resistances describing losses.

In this section, the partial elements' rigorous mathematical definitions as well as their approximations typically employed in a PEEC model are described and discussed.

A. Partial Inductance for Both Domains

Depending on the highest frequency of interest, the elements are differently formulated. The inductances for *quasi-static or low-frequency* solutions are

$$L_{p_{m,n}}^{QS} = \frac{\mu_0}{4\pi} \frac{1}{A_m A_n} \int_{V_m} \int_{V_n} \frac{\hat{\mathbf{t}}_m \cdot \hat{\mathbf{t}}_n}{|\mathbf{r}_m - \mathbf{r}_n|} dV_m dV_n \qquad (20)$$

where $\hat{\mathbf{t}}_m$ and $\hat{\mathbf{t}}_n$ represent the unit vectors in the direction of the current flow and S_m and S_n are the current conductor cross-section areas for the current. Further, V_m and V_n represent the threefold integrals for the conductor volumes. The inductances are called to be partial since a single partial inductance does not result in a meaningful inductance result.

The analytical evaluation of the partial inductances (20) is possible for rectangular Manhattan shapes [6]. This approach has several advantages since it results in nonsingular partial self-inductance and it can handle large aspect ratio shapes which would be very costly using numerical techniques.

The most complete (*full wave, full spectrum*) solution requires that the exponential term is included under the integral as

$$L_{p_{m,n}}^{FW}(j\omega) = \frac{\mu_0}{4\pi} \frac{1}{A_m A_n} \int_{V_m} \int_{V_n} \hat{\mathbf{t}}_m \cdot \hat{\mathbf{t}}_n \frac{e^{-j\beta R_{m,n}}}{|\mathbf{r}_m - \mathbf{r}_n|} dV_m dV_n \qquad (21)$$

where $\beta = \omega/c_0$ The exponential $e^{-j\beta R_{m,n}}$ is the factor accounting for the propagation delay effects taking place between the two volumes. Rigorously, the delay exponential function is fully involved in the integration process, since the propagation effects are connected to the whole points in the volumes V_m, V_n.

We observe that using (21) requires the recomputation for the partial inductances at each frequency sample, which is expensive. The numerical evaluation of (21) can be performed using numerical integration using methods like the Gauss quadrature. Of course, the computational effort increases linearly with the number of frequency samples required and, as usual, the singularities for the self-term have to be taken care of. Unfortunately, a full wave solution can be obtained only for limited cases of (21).

A direct improvement of (20) can be obtained by considering a unique time delay between the volumes, to extract the exponential delay from the integral. Usually, the delay $\tau_{cc} = R_{m,n}^{CC}/c_0$ corresponding to the distance $R_{m,n}^{CC}$ between the volume centers is chosen. Thus, assuming $R_{m,n} \simeq R_{m,n}^{CC}$ in (21), the center-to-center (CC) approximation of the partial inductance $L_{p_{m,n}}^{FW}$ is obtained

$$L_{p_{m,n}}^{CC}(j\omega) = e^{-j\beta R_{m,n}^{CC}} \frac{\mu_0}{4\pi A_m A_n} \int_{V_m} \int_{V_n} \frac{\hat{\mathbf{t}}_m \cdot \hat{\mathbf{t}}_n}{|\mathbf{r}_m - \mathbf{r}_n|} dV_m dV_n$$

$$= e^{-j\beta R_{m,n}^{CC}} L_{p_{m,n}}^{QS}. \qquad (22)$$

In the recent work [100], it has been shown that the Taylor series approximation can be used to compute the full-wave partial elements. Using the Taylor series of the exponential around zero

$$e^{-j\beta R} = \sum_{l=0}^{\infty} \frac{(-j\beta)^l}{l!} R^l \approx 1 - j\beta R - \frac{\beta^2 R^2}{2} + j\frac{\beta^3 R^3}{6} + \dots. \qquad (23)$$

leads to the expanded version of the partial inductance $L_{p_{m,n}}^{FW}$

$$L_{p_{m,n}}^{FW} \cong \frac{\mu_0}{4\pi} \frac{1}{S_n S_m} \sum_{l=0}^{N} \left[\frac{(-j\beta)^l}{l!} \int_{V_n} \int_{V_m} R^{l-1} dV_m \, dV_n \right]. \qquad (24)$$

A better approximation for far-apart cells is obtained by taking the center distance $R_{m,n}/c_0$ delay between the two cell centers outside of the integral and then expanding the exponential $e^{-j\beta(R-R_{m,n})}$. This leads to the following approximation of the partial inductance $L_{p_{m,n}}^{FW}$:

$$L_{p_{m,n}}^{FW} \cong \frac{\mu_0}{4\pi} \frac{1}{S_n S_m} e^{-j\beta R_{m,n}}$$

$$\cdot \sum_{l=0}^{N} \left[\frac{(-j\beta)^l}{l!} \int_{V_n} \int_{V_m} \frac{(R - R_{m,n})^l}{R} dV_m \, dV_n \right]. \qquad (25)$$

For TD analyses, (20) can be used as is since it is frequency independent. The TD counterpart of (21) can be recovered via the inverse Fourier transform (IFT) but is computationally expensive since it requires the computation of the partial element at many frequency samples over a wide frequency range. The CC approximation (22) can be easily translated to the time domain as

$$L_{p_{m,n}}^{CC}(t) = L_{p_{m,n}}^{QS} \delta\left(t - \frac{R_{m,n}^{CC}}{c_0}\right) \qquad (26)$$

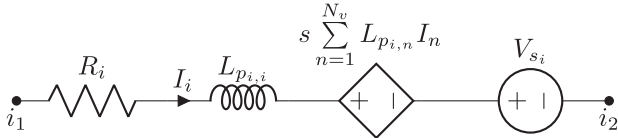where $\delta(t)$ denotes the delta Dirac function.

Fig. 7.   PEEC equivalent circuit model of a conductive elementary volume.

Fig. 8.   PEEC equivalent circuit of a dielectric elementary volume.

More recently, rigorous TD expressions for partial inductances and coefficients of potentials have been proposed in [101], [102], and [103] assuming rectangular Manhattan shapes. An effective way to recover TD partial inductances for nonorthogonal shapes of the volumes is to use the modified numerical inversion of the Laplace transform [104] that uses the Cauchy's theorem.

B. Coefficients of Potential

There is a great similarity between the coefficient of potential partial elements and the partial inductance in Section IV-A.

In the case of good conductors, it is assumed that the charge is on their surface because it moves to the surfaces at a fast rate [57]. Also in the case of homogeneous dielectrics, the polarization charge can be assumed to be only on their surface. Under the quasi-static approximation, the basic form of the coefficient of potential is

$$P_{m,n}^{QS} = \frac{1}{4\pi\epsilon_0} \frac{1}{S_m S_n} \int_{S_m} \int_{S_n} \frac{1}{|\mathbf{r}_m - \mathbf{r}_n|} dS_m dS_n \qquad (27)$$

where, in this case, $S_{m,n}$ represents the area surface of the cells. The full-wave coefficient of potential is

$$P_{m,n}^{FW} = \frac{1}{4\pi\epsilon_0} \frac{1}{S_m S_n} \int_{S_m} \int_{S_n} \frac{e^{-j\beta R_{m,n}}}{|\mathbf{r}_m - \mathbf{r}_n|} dS_m dS_n. \qquad (28)$$

In lossy dielectrics, such as silicon, due to the reduced value of their conductivity, the charge is not restricted to its surface, e.g., the relaxation time is not as small as in standard conductors. In this case, the coefficients of potential have to be computed as a double-folded volume integral

$$P_{m,n}^{QS} = \frac{1}{4\pi\varepsilon_0 V_m V_n} \int_{V_m} \int_{V_n} \frac{1}{|\mathbf{r_m} - \mathbf{r_n}|} dV_m dV_n. \qquad (29)$$

In [105], analytical formulas are presented for (28) under the hypothesis of orthogonal geometries.

V. MODELING OF CONDUCTORS, DIELECTRICS, AND MAGNETIC MATERIALS

Over the years, the PEEC method has had many improvements concerning the possibility of modeling materials of different types. This section briefly revised the models which have been introduced since the beginning.

A. Conductors

In its original 1974 version [8], the PEEC method only considered conductors. Fig. 7 shows an example of the equivalent circuit of an elementary volume of a conductor. Conductive dispersive materials are in use today like graphene. PEEC modeling of graphene interconnects has been presented in [106] and [107].
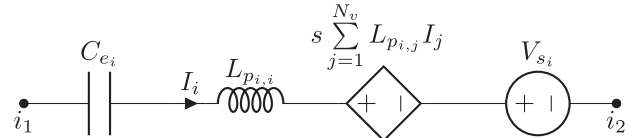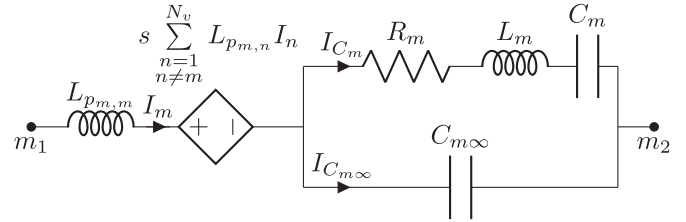

Fig. 9.   PEEC equivalent circuit of a dielectric elementary volume of Lorentz type.

B. Dielectric Materials

The equivalent circuit model of lossless ideal dielectrics was introduced in 1992 making it possible to model realistic interconnects [12]. The polarization of the dielectric is modeled by the so-called excess capacitance which, assuming a Manhattan-type mesh, for a cell of length ℓ and cross-section S, can be written as

$$C_e = \frac{\varepsilon_0 (\varepsilon_r - 1) S}{\ell} \qquad (30)$$

where ε_r is the relative permittivity of the dielectric. It is to be noticed that polarization currents are bound to the dielectric and generate magnetic fields and interact exactly as electrical currents. The equivalent circuit of an elementary volume of a dielectric is sketched in Fig. 8.

With the increase of the frequencies of interest, it has become more and more important to model the dispersive and lossy behavior of dielectrics. PEEC models of dispersive dielectrics of Debye and Lorentz type have been presented in [108]. Fig. 9 shows an example of the equivalent circuit of a dielectric elementary volume of Lorentz type.

PEEC models of lossy dielectrics, like silicon, and anisotropic dielectrics have been presented in [105] and [109], respectively. Finite-sized piecewise homogeneous dielectrics easily require massive equivalent circuits. Novel compact models of finite-size dielectrics that are based on the surface equivalence principle and the quasistatic assumption are presented in [110] and [111].

C. Magnetic Materials

The modeling of magnetic materials has been addressed first by considering the magnetization and the constitutive

$$\mathbf{B}(\mathbf{r}, s) = \frac{\mu_0 \mu_r}{\mu_r - 1} \mathbf{M}(\mathbf{r}, s) \qquad (31)$$

which, being the flux density divergence-less, can be rewritten as

$$\nabla \times \mathbf{A}(\mathbf{r}, s) = \frac{\mu_0 \mu_r}{\mu_r - 1} \mathbf{M}(\mathbf{r}, s). \qquad (32)$$
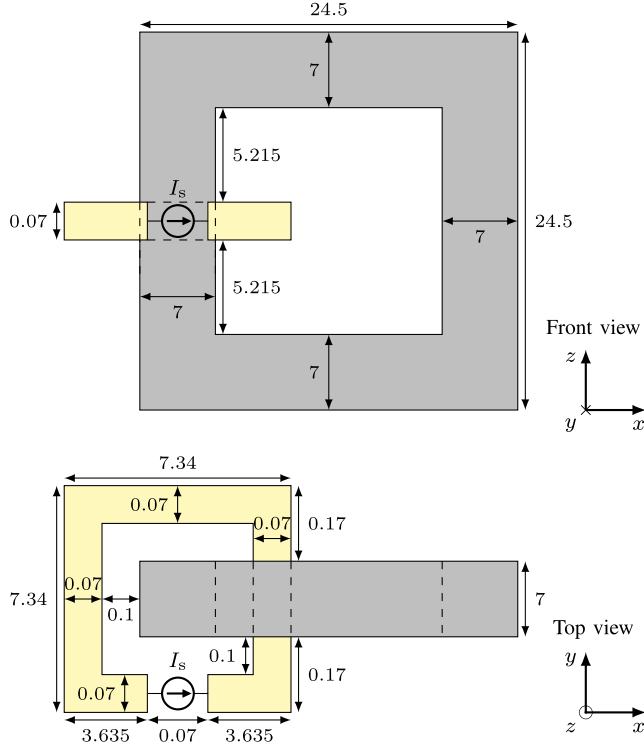
Fig. 10.   Closed magnetic circuit (not to scale). All dimensions are in mm.

Fig. 11.   Closed magnetic circuit. (a) Time evolution of B_z and H_z at the center of the excited limb. (b) B_x versus H_x at the same point.

Enforcing (32) in each direction of the Cartesian reference yields an additional set of equations

$$\mathbf{DI}(s) + \mathbf{TM}(s) = -\mathbf{GI}_s(s). \qquad (33)$$

Furthermore, the magnetic vector potential has an additional contribution due to the magnetization resulting in a modified KVL

$$-\mathbf{A}^T \mathbf{\Phi}(s) + \mathbf{RI}(s) + s\mathbf{L}_p(s)\mathbf{I}(s) + s\mathbf{L}_m(s)\mathbf{M}(s) = \mathbf{V}_s(s). \qquad (34)$$

Hence, the set of equations to be solved reads

$$\begin{bmatrix} s\mathbf{P}^{-1} & \mathbf{A} & \mathbf{0} \\ \mathbf{A}^T & -[\mathbf{R} + s\mathbf{L}_p] & -s\mathbf{L}_m \\ \mathbf{0} & \mathbf{D} & \mathbf{T} \end{bmatrix} \cdot \begin{bmatrix} \mathbf{\Phi} \\ \mathbf{I} \\ \mathbf{M} \end{bmatrix} = \begin{bmatrix} \mathbf{I}_s \\ -\mathbf{V}_s \\ -\mathbf{GI}_s \end{bmatrix}. \qquad (35)$$

This formulation was proposed for the first time in [112]. Under the quasi-static hypothesis, rigorous analytical formulas are proposed in [113] for integrals accounting for flux density due to current and magnetization densities for the Manhattan-type discretizations. The formulation presented in [112] has been extended in [114] for modeling 3-D magnetic plates for low-frequency magnetic shielding problems. An augmented PEEC formulation has been proposed in [106] to model dispersive and lossy linear magnetic materials again under the quasi-static hypothesis. A novel PEEC formulation that is able to handle 3-D nonlinear problems has been proposed in [115]. A behavioral magnetostatic hysteresis model has been implemented in a PEEC environment and presented in [116]. Fig. 10 shows an example of a closed magnetic circuit that is excited by a loop driven by an enforced current. The time evolution of the B and H z-components, probed at the center of the excited limb, are presented in Fig. 11 along with the corresponding B-H curves.

VI. PEEC SOLVERS

The equivalent circuits generated by the PEEC method are well suited to be analyzed in both the frequency and the time domains.

A. Frequency Domain Solvers

Frequency domain solvers solve the MNA set of equations (17) over a set of frequency samples $s_k = j\omega_k, k = 1, \dots, N_f$, in the frequency bandwidth of interest.

For small problems, with a number of DoFs not exceeding 30 000, the solution can be addressed using direct solvers, e.g., the LU decomposition. The direct solution can be accelerated by resorting to the multiscale block decomposition and the adaptive cross approximation (ACA) technique [117], as described in [118], [119], [120], and [121].

Typically, the filling of partial inductances and coefficients of potential matrices, $\mathbf{L}_p(j\omega)$ and $\mathbf{P}(j\omega)$, respectively, is computationally heavy since they must be computed at each frequency. Their computation can be accelerated by resorting to the fast multipole method (FMM) [122]. Indeed, these matrix entries fluctuate slowly with frequency and have a polynomial behavior that can be efficiently interpolated by the Lagrange interpolation scheme, as was shown in [123]. In [124], an effective methodology for the interpolation in space of the partial inductances

required by the PEEC method is developed. It makes use of the cubic spline interpolation method, that, under the hypothesis of cubic meshed regions, guarantees always a significant speed-up without loss of accuracy.

For large problems, iterative solvers become mandatory because matrices become so large that they cannot be stored. In this case, matrix-vector products must be computed. An approach that is based on the compression of the partial inductance matrix utilizing the QR decomposition of the far coefficients submatrices is proposed in [125]. To speed up the matrix-vector products, the translational invariance of elementary magnetic and electric field interactions can be exploited. In particular, in [126] a method is proposed that allows one to exploit providing significant memory saving and an excellent improvement of the computation performances. This method was then applied to inductance extraction in [127]. A Tucker-enhanced and FFT-accelerated version of the method has been proposed for capacitance and inductance extraction in [128] and [129], respectively. Such an approach has been applied to PEEC models of power electronics applications in [18] and [19].

The ACA coupled with hierarchical matrix (H-matrix) arithmetics [130] can also provide an effective method to increase the size of the largest solvable problems. This approach has been investigated in the framework of the PEEC method in [131] and [132].

1) dc and Low-Frequency Solution: A rigorous *dc* solution of PEEC models of conductors has been proposed in [133] using a two-step process. First, a magnetostatic problem is analyzed by solving a purely resistive network providing the currents in the circuit. Then, an electrostatic problem is solved by enforcing the neutrality of each conductor, which is completely disconnected from the others, and using the voltage drops known from the magnetostatic problem as a boundary condition. This methodology has then been extended in [134] to PEEC models consisting of conductors but also of ideal dielectrics and magnetic materials. Fig. 12 shows the geometry of a loop inductor and the corresponding distribution of node *dc* potentials.

2) PEEC Models With Dyadic Green's Function: The *tout-court* application of the PEEC method to problems involving large layered media, as they occur in PCB modeling or in problems involving transmission lines over or buried in the ground, would require the dielectric to be discretized using a 3-D grid. Thus, it would end up in a large system of algebraic equations with a computational cost that easily becomes prohibitive. A valuable alternative for such problems is represented by the use of the dyadic Green's functions for layered media (DGFLM). This formulation requires the discretization only of conductors, while the Green's functions include the features of the multilayer substrate. A novel numerical solution for the mixed potential integral equation for layered media using the PEEC method has been presented in [135]. The same concept has been used for modeling patch antennas [136], PI problems, multilayered PCBs [137], [138], [139], [140], and 3-D IC/packaging analysis [141], [142].

When the PEEC method is adopted to analyze lightning transients in wire/plate structures in the air and lossy-ground space, it
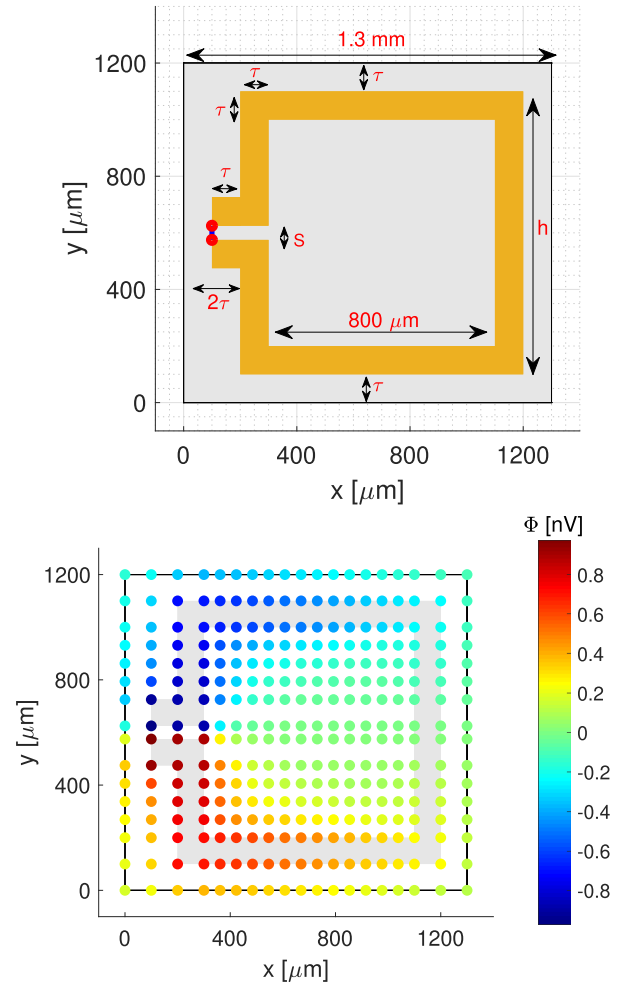
Fig. 12.   Loop inductor and *dc* node potential distribution.

is necessary to evaluate the Green's functions for layered media for both vector and scalar potentials for source and field points in any of these two layers. This approach has been applied to address both transient current and voltage in a variety of structures with arbitrarily oriented lines and plates [143], [144], [145], [146], [147], [148], [149], [150], [151], [152], [153].

Time domain solvers: Full-wave PEEC models can be analyzed in the time domain using three different approaches which are as follows.
1) Time-stepping methods.
2) Inverse Fourier transform (IFT)
3) Numerical inversion of the Laplace transform (NILT).

3) Time Stepping Methods: The enforcement of the Kirchhoff voltage and current laws to the PEEC model yields the following set of neutral delayed differential equations (NDDE) [57]

$$\mathbf{C}(t)\frac{d\mathbf{x}(t)}{dt} = -\mathbf{G}(t)\mathbf{x}(t) + \mathbf{B}\mathbf{u}(t). \qquad (36)$$

The vector of the unknowns $\mathbf{x}(t) \in \Re^{n_u \times 1}$ is given as

$$\mathbf{x}(t) = [\mathbf{i}(t) \quad \phi_{sr}(t) \quad \phi_i(t) \quad \mathbf{v}_d(t) \quad \mathbf{q}_s(t)]^T \qquad (37)$$

where $\mathbf{i}(t)$ are the branch currents, $\phi_{sr}(t)$ are the scalar potentials for surface nodes, $\phi_i(t)$ are the scalar potentials for internal nodes, $\mathbf{v}_d(t)$ are the excess capacitance voltages for dielectric branches, and $\mathbf{q}_s(t)$ represent the surface charges. Furthermore, the state space matrices $\mathbf{C}(t)$, $\mathbf{G}(t)$, and $\mathbf{B}$ are

$$\mathbf{C}(t) = \begin{bmatrix} \mathbf{L}_p(t)* & 0 & 0 & 0 & 0 \\ 0 & 0 & 0 & 0 & \mathbf{M}^T \\ 0 & 0 & 0 & 0 & 0 \\ 0 & 0 & 0 & \mathbf{C}_d & 0 \\ 0 & 0 & 0 & 0 & 0 \end{bmatrix} \tag{38}$$

$$\mathbf{G}(t) = \begin{bmatrix} \mathbf{R} & \mathbf{A}_s & \mathbf{A}_i & \mathbf{\Gamma} & 0 \\ -\mathbf{A}_s^T & \mathbf{G}_{le} & 0 & 0 & 0 \\ -\mathbf{A}_i^T & 0 & 0 & 0 & 0 \\ -\mathbf{\Gamma}^T & 0 & 0 & 0 & 0 \\ 0 & -\mathbf{M} & 0 & 0 & \mathbf{P}(t)* \end{bmatrix} \tag{39}$$

$$\mathbf{B} = \begin{bmatrix} \mathcal{I} & 0 \\ 0 & \mathcal{I} \\ 0 & 0 \\ 0 & 0 \\ 0 & 0 \end{bmatrix} \tag{40}$$

where $*$ represents the convolution operator, $\mathbf{C}_d$ is the excess capacitance matrix [13], $\mathbf{R}$ is the branches resistance matrix, $\mathbf{A}_s$ is the incidence matrix for the surface nodes, $\mathbf{A}_i$ is the incidence matrix for the internal nodes, $\mathbf{\Gamma}$ is the dielectric region selection matrix, $\mathbf{M}$ is the surface-to-node reduction matrix, and $\mathbf{G}_{le}$ is the load conductance matrix (assuming by now for simplicity that only resistive lumped elements are connected to the PEEC model).

Also, the time-dependent partial inductance matrix $\mathbf{L}_p(t)$ and the coefficient of potential matrix $\mathbf{P}(t)$ are considered as impulsive, that is

$$\mathbf{L}_p(t) = \mathbf{L}_p^{DL}\delta(t) + \sum_{i=1}^{N_{L_p}} \mathbf{L}_p^D \delta(t - \tau_{cc,i}) \tag{41a}$$

$$\mathbf{P}(t) = \mathbf{P}^{DL}\delta(t) + \sum_{q=1}^{N_P} \mathbf{P}^D \delta(t - \tau_{cc,q}), \tag{41b}$$

where the superscripts DL and D stand for delay-less and delayed, respectively; N_{L_p} is the number of significant delays between elementary volumes while N_P is the number of significant delays between elementary surfaces; $\tau_{cc,i} = R_{cc,i}/c_0$, $i = 1, \ldots, N_{L_p}$ and $\tau_{cc,q} = R_{cc,q}/c_0$, $q = 1, \ldots, N_P$ denote the delays between the centers, identified by $R_{cc,i}$ and $R_{cc,q}$, respectively, of the spatial supports of the basis functions of currents and charges; c_0 is the speed of the light in the background medium.

Finally, the source vector $\mathbf{u}(t)$ is given as

$$\mathbf{u} = \begin{bmatrix} \mathbf{v}_s(t) \\ \mathbf{i}_s(t) \end{bmatrix} \tag{42}$$

where $\mathbf{v}_s(t)$ and $\mathbf{i}_s(t)$ are the voltage and current sources, which are applied to branches and nodes, respectively.

The solution of (36) has been addressed in [154] experimenting with different temporal basis functions.
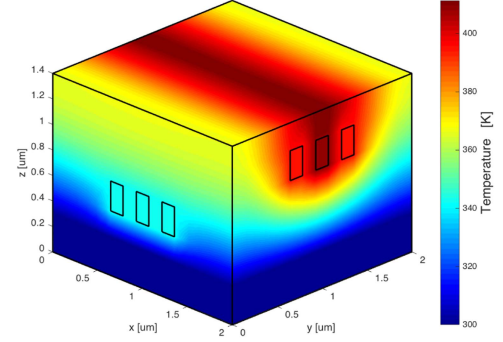
Fig. 13. Transient temperature map on the surface of a multilevel on-chip interconnect.
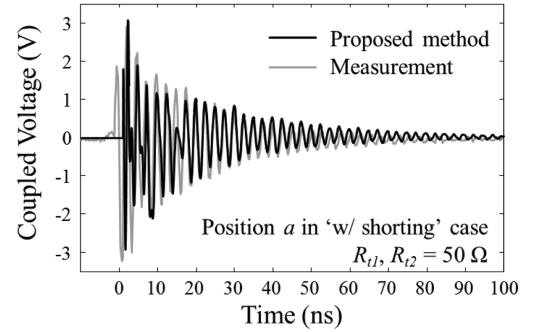
Fig. 14. Computed and measured ESD coupling waveform (see [159] for the details).

Time domain PEEC modeling has been combined with a thermal solver to perform an electrothermal analysis in [105]. Fig. 13 shows the surface temperature of a multilevel chip interconnect [155].

In [156], the analysis of delayed PEEC models has been accelerated by using the waveform relaxation technique. An innovative time domain digital wave PEEC solver has been presented in [157] under the quasi-static hypothesis.

PEEC time domain solvers have been used to analyze ESD problems in [158] and [159]. Fig. 14 shows the calculated and measured voltage waveforms induced by a 2-kV ESD event.

a) Time domain stability issues: Stability has for a long time been a challenge for time domain methods [160]. It is an issue also for PEEC models like (36).

The stability analysis of solutions consists of two basic aspects.

First, the stability of the model, and thus, of its differential equation system, is to be considered. If the PEEC model is unstable, its numerical solution is generally unstable. However, sometimes, one can obtain a stable numerical solution by using a numerical scheme whose region of absolute stability allows one to obtain a stable solution even for unstable models, but it is not granted that this solution represents well the physical response of the system.

In [161], it is shown that the discretization of PEEC models can lead to differential equations with unstable solutions. A stabilization scheme is introduced using so-called split cells. Damping resistors introduced in parallel to self-inductances in

the standard PEEC have been suggested as an effective tool for the stabilization of the solution [162]. This modification, although it does not increase the number of unknowns, since it increases the damping, may affect the accuracy of the results.

The accuracy in the computation of partial elements may have an impact on the stability. We will distinguish two cases:

1) quasi-static (QS) PEEC models (propagation delays are neglected); PEEC models are described by *RLC* equivalent circuits and, Kirchhoff laws lead to ODEs;
2) full-wave PEEC models (propagation delays are considered; they are described by *RLC* circuits with delayed sources and Kirchhoff laws lead to NDDEs.

In both cases, PEEC model stability is significantly affected by the mesh. Indeed, the aspect ratios of the elementary volumetric and surface regions impact the accuracy of the computation of partial elements. It happens when they are computed using analytical formulas, which is possible under the quasi-static hypothesis and using orthogonal meshes. Double precision floating point (IEEE Standard 754), introduces a truncation error in their computation. It is known that for cells with extreme form factors (the ratios between the sizes of the cells) or for extreme ratio distance/size, the truncation error might be so large that the computation of the partial elements is completely dominated by the numerical error. In [19], guidelines for using the analytical formulas are provided depending on the sizes of the elementary domains and their distances.

Then, as pointed out in [163], [164], and [165], the CC approximation is recognized as one further cause driving the model to instability. In [163], a low pass filter (LPF) is used for each partial element, and then the state-space description of the resulting delay-free system is constructed and the stability is assessed by checking the eigenvalues of the system matrix. However, to match the behavior at sufficiently high frequencies, the order of each LPF has to be as high as 38, resulting in quite a significant increase in the number of DoFs. This limitation is mitigated in [166], where time domain models of integrals of Green's functions are proposed leading to full-spectrum convolution macromodeling.

All these types of approximations may lead to right-half-plane unstable poles causing the so-called *late time instability*. It is important to observe that the unstable poles are very weak in amplitude and typically have a very large imaginary part, so they do not impact significantly the low frequencies. Fig. 15 shows an example of poles of a zero thickness conductor PEEC model, 10-cm long and 2-cm wide. In particular, the poles have been computed first neglecting all the delays (Quasi-static) and then using a first-order Taylor expansion to approximate the exponentials in a polynomial form.

To establish a priori the stability of a PEEC model, it would be necessary to compute explicitly its poles. Due to the theoretical complexity of a time-delayed system like PEEC, however, the existing stability tests are all either sufficient or necessary, but not both. The analytic computation of poles is possible only in a few simple cases or when delays are neglected. On the other hand, sufficient conditions hold under strong assumptions, considering only a reduced number of delays, and with a significant computational cost, making their utility questionable [167], [168],
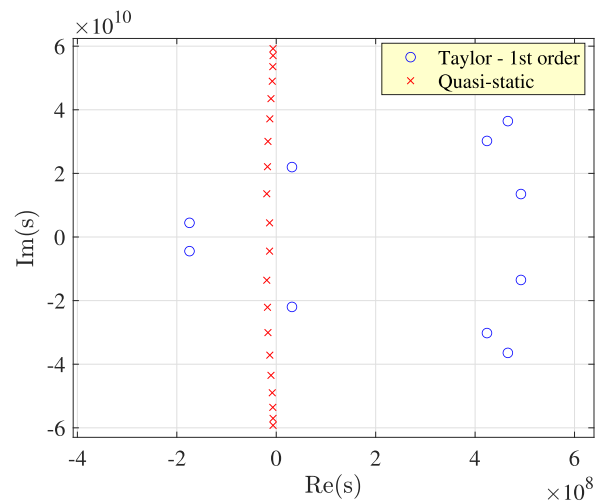

Fig. 15.	Stable and unstable poles of delayed PEEC models.

[169], [170]. An effective pole-based stability test is proposed in [171].

Second, an unstable solution may be caused by the numerical method itself. Different numerical methods have different regions of absolute stability. They can be described as A-stable, L-stable [160].

The influence of the numerical method features on the stability of full-wave PEEC models has been investigated in [172], where the P-stability has been defined as a criterion for choosing an appropriate numerical method. Bellen et al. [167] studied a PEEC model with one single delay, and propose a sufficient-condition test based on checking some matrix-norm inequalities. Extension of this method to models with more delays, however, remains unclear. In general, the backward Euler (BE) and Lobatto III-C have also been proposed as suitable numerical methods for the PEEC method.

a) The Inverse Fourier Transform: The easiest way, although not the most efficient one, to obtain TD responses of PEEC models is represented by the use of the FT applied to the FD results made available by an FD solver of the equations in (17) over a pertinent set of frequency samples $s_k = j\omega_k, k = 0, \ldots, N_f$. This approach has some disadvantages as follows.

1) The frequency response must be computed over the entire bandwidth of interest in order to evaluate the time domain counterpart; the maximum frequency for which the model is accurate based on some criteria is decided by the mesh; frequency responses at higher frequencies are less accurate. This will only impact the accuracy of the IFT computed waveforms, not the stability because the IFT entails a weighted sum of multiple contributions and it is not affected by the stability problems of time-stepping methods.
2) If the sources to the system are waveforms with sharp edges (such as a pulse with sharp rise/fall times), a very large number of frequency points would be required in order to avoid aliasing problems [173].
3) Nonlinear materials or lumped elements cannot be easily handled.

In addition, in order to achieve accurate results, it is necessary to let the energy vanish at the end of the simulation. This means that the signal exciting the system as well as the associated response have to be band-limited in frequency and time. This poses a serious limitation in computing the step response since the FT of a step function is not band-limited. As an approximation, FT of a square (more likely trapezoidal) pulse going back to zero once the steady-state output is reached can be used. Additional simulation time is required to ensure that the system response goes to zero as well. This results in a larger number of frequency points where the solution of the system equations is needed. Moreover, the IFT needs the *dc* solution of the system which is a well-known issue for EM models (see Section VI-A1).

a) The Numerical Inversion of the Laplace transform: The numerical inversion of the Laplace transform (NILT) technique represents a valid alternative to time-stepping solvers. This technique, introduced in the early '70s of the last century [174], has gained more and more interest in the TD characterization of linear-time-invariant (LTI) systems. Essentially, given the state vector $\mathbf{X}(s)$ of an LTI system expressed in the complex frequency domain in the form

$$\mathbf{N}(s)\mathbf{X}(s) = \mathbf{U}(s) \tag{43}$$

as it appears in (17), the well-known Laplace inverse transform can express its TD counterpart as [175]

$$\mathbf{x}(t) = \frac{1}{j2\pi} \int_{\alpha-j\infty}^{\alpha+j\infty} \mathbf{X}(s)e^{st}ds \tag{44}$$

where $\alpha > \Re e(p_k) \; \forall p_k$, where p_k are the poles of $\mathbf{X}(s)$. The Laplace inverse integral can be approximated by replacing st with z and e^z with its $[N/M]$ Padé approximant [176] $\xi_{N,M}(z)$, finally employing the Cauchy theorem of residues [177]. Assuming M an even integer, the NILT approximation for the TD state vector results in

$$\mathbf{x}(t) \simeq -\frac{1}{t} \sum_{i=1}^{M/2} 2\mathrm{Re}\left[K_i\mathbf{X}(s)\right]_{s=\frac{z_i}{t}} \tag{45}$$

being z_i and K_i the Padé poles and residues, respectively. It is evident from (45) that the knowledge of the system's poles is not required to build the transient waveforms associated with the corresponding Laplace domain quantities. Moreover, the method's accuracy is not bounded by the time-step choice and, consequently, does not depend on the number of time samples employed. Furthermore, also the solution's stability of the solution is not affected by the time-step. Hence, the responses of LTI PEEC models remain always stable when reproduced by NILT.

For illustrative purposes, Fig. 16 shows two different sets of poles z_i/t corresponding, respectively, to the choices $M = 6$ and $M = 12$, with $N = M - 2$. The two sets are computed over the same time window $[1-5]$ ns.

It is evident that, as time t increases, each set of poles approaches the origin of the complex plane, causing a loss of accuracy with the evaluation time. To mitigate this limitation, a modified NILT, known as NILTn, has been recently proposed in the framework of TD simulation of multiconductor transmission lines (MTL) [178]. The MNA representation of full-wave PEEC
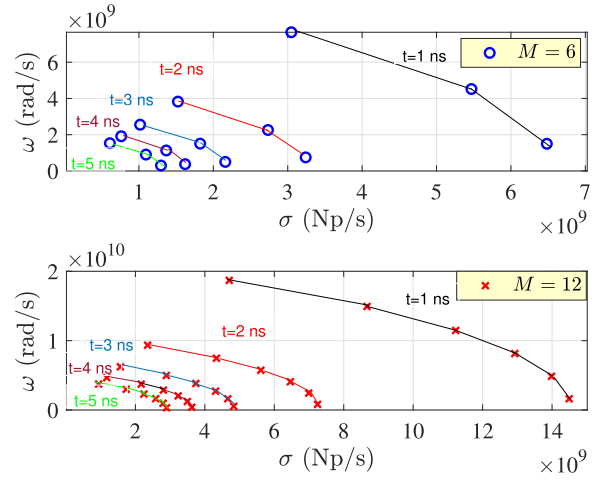
Fig. 16. Two Padé poles sets moving in the complex plane as the evaluation time increases.
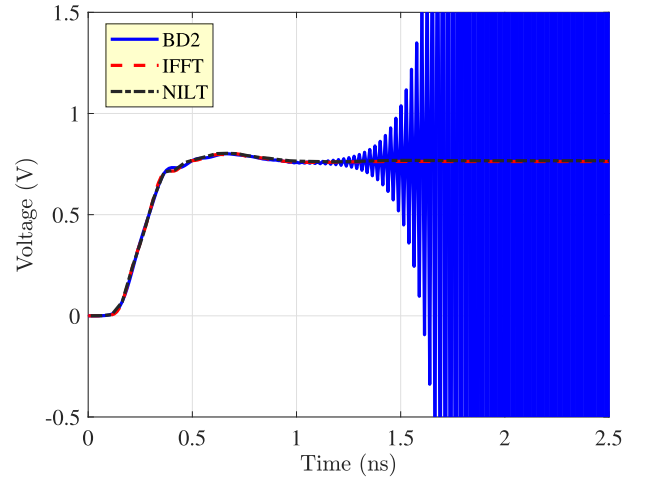
Fig. 17. Power-divider port voltage computed with NILT: a comparison with well-established methods.

models in the Laplace domain (43), being the NILT scheme easily applicable. The NILT technique has been applied for the first time to retarded PEEC models in [179], where its stability properties are emphasized when compared to time-stepping methods applied to the resolution of retarded PEEC models. For illustrative purposes, in Fig. 17 the port voltage response of a power divider, a typical microstrip device, is depicted, assuming a trapezoidal waveform at its feeding port. The EM model of the structure has been built through the PEEC model considering the propagation delays, giving rise to an LTI retarded system. The NILT results agree with those of the IFFT, while those obtained through the BD2 time-stepping scheme exhibit clear late-time stability issues ($t > 1$ ns).

Subsequently, in [180], the modified NILTn has been successfully employed for retarded PEEC models showing accuracy improvements and reduced computational costs.

It is worth noticing that the NILT approach does not compute the response based on the singularities of the PEEC model, but

rather on the relevant Padé matrix. Hence, the eventual right-hand side (*RHS)* unstable poles of the PEEC model are automatically filtered and do not impact the accuracy of the solution.

VII. COMPARISON WITH THE METHOD OF MOMENTS

Both the MoM and PEEC integral equation-based approaches are using what is known as the *weighted residual method* (MWR or WRM) [181], [182] to discretize the formulation into numerical solutions. Originally, the mathematical MoM notation was part of fundamental WRM techniques. As pointed out in [181], WRM applies to the solution of both differential as well as integral equation-based problems. Hence, WRM can be used for both approaches we consider here.

To give a unique name to the MoM considered here, we call it the Z-MoM method since the formulation leads to an impedance formulation. Of course, the Z-MoM name can also be used for the time domain versions since the basic equations are the same. Further, the Z-MoM method was devised in a time before PEEC [4]. The key difference between the two methods is in the fundamental derivation of the solution which results in different unknowns. The derivation of the PEEC method is given in Section II, where it is clear that the unknowns are both the potential Φ and the current $\mathbf{I}$, which leads the equations in the MNA form (17) which can be implemented with other SPICE type circuit domain models.

The Z-MoM method is based on the same fundamental integral equation (4) as is PEEC. However, the charge or potential variable is eliminated using the continuity equation (5). This results in the impedance formulation of the Z-MoM method.

Another difference exists between Z-MoM and PEEC meshing approaches. The main issue is based on the fact that Z-MoM has mesh cells only for the current variables, while PEEC requires appropriate, separate cells for both the potential as well as the currents, as is obvious from the formulation in Section II. It is clear that the inductive and resistive partial elements connect between nodes while the capacitive cells are connected to the nodes. This applies to all types of cells including nonorthogonal meshing. In the original PEEC method, the meshing was mostly based on orthogonal bricks or hexahedron volumes and rectangular cells or quadrilaterals to mesh the surfaces. The Z-MoM mostly uses triangular meshes for surfaces [94] and tetrahedral meshes for volumes [95]. This has led to the development of dedicated basic functions, known as the RWG basis functions for triangles [94] and the Schaubert–Wilton–Glisson (SWG) basis functions for tetrahedral volumes [95].

The use of triangular/tetrahedral cells allows for an accurate model of complex geometries. However, easily results in a large number of cells and unknowns when compared to quadrilateral meshes.

An important issue for the Z-MoM formulation is the so-called low-frequency breakdown. This is because the low-frequency response including the *dc* [183] solution is poor or missing. This high-pass behavior is an important issue for the solution of some EMC, SI, and PI problems while it is not an issue for the solution of high-frequency antenna problems. The Z-MoM formulation has been improved by resorting

to augmented formulations which also assume the charges as unknowns, and also by adopting suitable scalings to improve the condition of the system [184], [185]. In [186], it has been shown that the MNA form of PEEC models attenuates the low-frequency breakdown even for problems that do not have closed loops which also results in *dc* solutions.

VIII. COMPUTATIONAL COMPLEXITY OF PEEC MODELS

Being an integral equation-based method, similar to MoM, the solution of PEEC models in both the frequency and time domains for quasi-static models requires the solution of a block-dense linear system. In the frequency domain, small problems, with a number of unknowns $N < 30\,000$, can be solved with direct solvers. They involve a factorization step followed by a solve step. The factorization step comprises an LU factorization or QR factorization, which is generally computationally very expensive. Further, direct solvers are advantageous when one is interested in multiple RHSs. A naive direct solver costs $O(N^3)$, which is prohibitively resource-demanding for large system sizes. To reduce the computational complexity, fast methods are used. Many dense matrices arising out of N-body problems possess a hierarchical low-rank structure. This low-rank structure is exploited to construct hierarchical matrices and hierarchical matrices-based fast direct solvers [130], [187], [188]. In the framework of the PEEC method, multiscale compressed techniques exploiting the low-rank nature of magnetic and electric field interactions have been presented in [118] and [189]. In [190], it has been shown that the storage requirements and computation time of these types of techniques scale as $O(N^{3/2})$ and $O(N^2)$, respectively, for asymptotically high frequency.

Hierarchical matrices have been used along with the PEEC method in [131], [191], and [192].

Larger-dimensional problems require iterative solvers that require repeated vector-matrix products with $O(N^2)$ complexity. It is possible to accelerate such vector-matrix products by resorting to methods, such as the FFM [193] and Barnes–Hut [194]. Using a multilevel approach, a $O(N\log N)$ computational complexity can be achieved asymptotically. Further, for fast convergence in problems with high-condition numbers, iterative solvers are coupled with a preconditioner. More recently, the FFT-based technique presented in [126] has been applied to the PEEC method in [18] and [19] allowing obtaining excellent memory and CPU time savings.

In the time domain, the system matrix is typically very sparse. This enables the efficient use of multifrontal techniques to perform the LU decomposition even for very large problems [195], [196], [197]. Nevertheless, when using time-stepping techniques, the RHS vector has to be updated at each time step requiring many matrix-vector products. In this case, FFT-based techniques can also be used to accelerate these matrix-vector products [198].

IX. MODEL ORDER REDUCTION OF PEEC CIRCUITS

The equivalent circuits generated by the PEEC modeling can be very large and easily require prohibitive storage and significant computing resources. Model order reduction (MOR)

techniques [199], [200] can be adopted to compress the $\mathbf{C}, \mathbf{G}, \mathbf{B}$ matrices in (36) preserving the accuracy of the reduced model at the ports. Equation (36) can be rewritten in the Laplace domain as

$$s\mathbf{C}(s)\mathbf{X}(s) = -\mathbf{G}(s)\mathbf{X}(s) + \mathbf{B}\mathbf{U}(s) \tag{46a}$$

$$\mathbf{Y}(s) = \mathbf{B}^T\mathbf{X}(s) \tag{46b}$$

$$\mathbf{C}(s) = \mathbf{C}_0 + \sum_{k=1}^{n_\tau} \mathbf{C}_k e^{-s\tau_k} \tag{46c}$$

$$\mathbf{G}(s) = \mathbf{G}_0 + \sum_{k=1}^{n_\tau} \mathbf{G}_k e^{-s\tau_k}. \tag{46d}$$

Several researchers have applied MOR techniques to examples of quasi-static PEEC models without retardation. See, for example [201], [202], and [203]. Procedures for reducing PEEC models with retardation were first proposed in [204] and [205]. Both of these references construct reduced-order models for the frequency domain transfer function. For PEEC models with retardation the transformed system matrix $\mathbf{Q}(s)$ contains many elements with factors of the form $e^{-s\tau}$ for some τ corresponding to a time delay (retardation) in the circuit. All of those papers expand each delay term in an infinite Taylor series. The authors in [204] used a single expansion point and applies asymptotic waveform (AWE) model reduction [206] to the resulting infinite order linear system. In that article, an example is included for which good approximations were obtained for low frequencies up to 1 GHz. Chiprout et al. [205] used complex frequency hopping (CFH), considered several expansion points, applied AWE to the infinite linear system obtained at each such point, and then combined the pole and residue information to obtain an approximation to the transfer function of the PEEC system. It includes examples showing that this method is accurate to approximate the transfer function of a system up to 4.8 GHz. A similar approach has been applied to a PEEC model in conjunction with an FFT grid representation in [207]. Furthermore, in [207], an equivalent first-order system is computed by means of a single-point Taylor expansion, and a corresponding orthogonal projection matrix is computed by means of a block Arnoldi algorithm [208], [209]. However, the NDDE formulation is not preserved. In [210], a readily parallelizable procedure is proposed for generating reduced-order frequency-domain models from general full-wave PEEC systems. Multiple expansion points and piecemeal construction of pole-residue approximations are adopted to approximate the transfer functions of the PEEC systems through an Arnoldi recursion. The reduction of equivalent first-order systems become computationally expensive and sometimes not feasible when large delays are involved since exponential terms with large delays need many terms in the Taylor expansion to be accurately approximated. The multipoint expansion [211] addresses this issue and is able to accurately reduce NDDE systems with large delays since a small expansion Taylor order can be used for each expansion point and the accuracy of the reduced model is increased by adding new expansion points. In [212], an adaptive algorithm is proposed to choose the expansion points, assuming that the order of the Taylor expansion is fixed for each expansion point.

When applying MOR techniques, in the simplest case, the reduced-order model can be obtained by performing a single-point expansion reduction. Denoting the orthogonal basis as $\mathbf{K} \in \Re^{n_u \times n_r}$, the reduced order system is given by

$$s\mathbf{C}_r(s)\mathbf{X}_r(s) = -\mathbf{G}_r(s)\mathbf{X}_r(s) + \mathbf{B}_r\mathbf{U}(s) \tag{47a}$$

$$\mathbf{Y}(s) = \mathbf{B}_r^T\mathbf{X}_r(s) \tag{47b}$$

$$\mathbf{C}_r(s) = \mathbf{C}_{r,0} + \sum_{k=1}^{n_\tau} \mathbf{C}_{r,k} e^{-s\tau_k} \tag{47c}$$

$$\mathbf{G}_r(s) = \mathbf{G}_{r,0} + \sum_{k=1}^{n_\tau} \mathbf{G}_{r,k} e^{-s\tau_k} \tag{47d}$$

where the following congruence transformations are used:

$$\mathbf{C}_{r,i} = \mathbf{K}^T\mathbf{C}_i\mathbf{K}, \quad i = 0, \dots, n_\tau \tag{48a}$$

$$\mathbf{G}_{r,i} = \mathbf{K}^T\mathbf{G}_i\mathbf{K}, \quad i = 0, \dots, n_\tau \tag{48b}$$

$$\mathbf{B}_r = \mathbf{K}^T\mathbf{B} \tag{48c}$$

$$\mathbf{L}_r = \mathbf{K}^T\mathbf{L} \tag{48d}$$

and $\mathbf{X}_r(s)$ is a vector containing the state variables in the reduced domain. To obtain a compact and accurate reduced order model over a wide frequency range it is important to construct the orthogonal basis $\mathbf{K}$. To this purpose, the Arnoldi algorithm [208] can be adopted because of its numerical reliability and robustness. Indeed, the Arnoldi algorithm is able to provide the orthogonal basis for the transfer function moments without computing these moments explicitly. Unfortunately, adapting the Arnoldi algorithm for NDDE systems is not straightforward, and, thus, the original NDDE system must be transformed into a suitable form for standard Arnoldi-based reduction. To address this issue, by expanding the exponential factors $e^{-s\tau_k}$ in a Taylor series form and using a companion form [213], an equivalent first-order system is computed. Then, the Arnoldi algorithm is applied to the first-order equivalent system, allowing the computation of the corresponding orthogonal projection matrix $\mathbf{K}$ for the original NDDE system, and a reduced NDDE system is finally obtained [213]. This single point expansion-based MOR algorithm for NDDE systems was proposed assuming $s = 0$ as an expansion point. If any other expansion point $s = s_1$, $s_1 \neq 0$ is selected, setting $s = s_1 + \sigma$, where s_1 is a frequency shift and σ is the new Laplace variable, the NDDE system (46a)–(46b) reads

$$\sigma\widehat{\mathbf{C}}(\sigma)\mathbf{X}(\sigma) = -\widehat{\mathbf{G}}(\sigma)\mathbf{X}(\sigma) + \mathbf{B}\mathbf{U}(\sigma) \tag{49a}$$

$$\mathbf{Y}(\sigma) = \mathbf{B}^T\mathbf{X}(\sigma) \tag{49b}$$

$$\widehat{\mathbf{C}}(\sigma) = \widehat{\mathbf{C}}_0 + \sum_{k=1}^{n_\tau} \widehat{\mathbf{C}}_k e^{-\sigma\tau_k} \tag{49c}$$

$$\widehat{\mathbf{G}}(\sigma) = \widehat{\mathbf{G}}_0 + \sum_{k=1}^{n_\tau} \widehat{\mathbf{G}}_k e^{-\sigma\tau_k} \tag{49d}$$
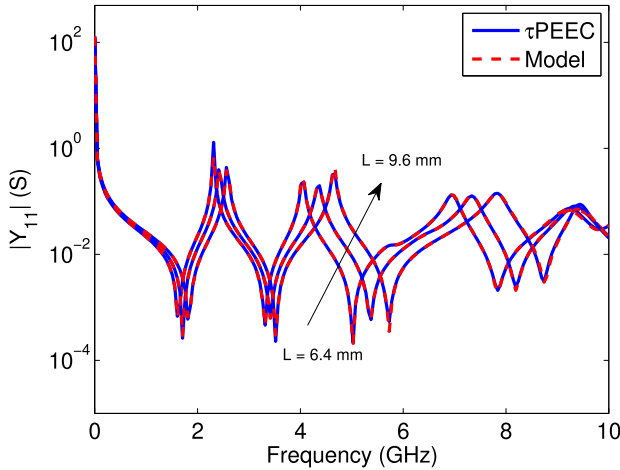
Fig. 18. Magnitude of the bivariate delayed ROMs of $\mathbf{Y}_{12}(s, L)$ ($L = \{6.4, 8, 9.6\}$ mm. See [216] for more details).

where

$$\widehat{\mathbf{C}}_0 = \mathbf{C}_0 \tag{50a}$$

$$\widehat{\mathbf{G}}_0 = \mathbf{G}_0 + s_1 \mathbf{C}_0 \tag{50b}$$

$$\widehat{\mathbf{C}}_k = \mathbf{C}_k e^{-s_1 \tau_k}, \ k = 1, \ldots, n_\tau \tag{50c}$$

$$\widehat{\mathbf{G}}_k = (\mathbf{G}_k + s_1 \mathbf{C}_k) e^{-s_1 \tau_k}, \ k = 1, \ldots, n_\tau \tag{50d}$$

and the algorithm described in [213] is applied. While the single-point MOR approach [213] is able to preserve the NDDE formulation, it may be not able to reduce NDDE systems with large delays since the reduction of equivalent first-order systems becomes computationally expensive and sometimes unfeasible because many terms in the Taylor expansion of the exponential terms with large delays are required to preserve the accuracy.

A more valuable alternative is represented by the multipoint expansion [211] that is able to accurately reduce NDDE systems with large delays since a reduced order of the Taylor expansion can be used for each expansion point while the accuracy of the reduced model is achieved by adding new expansion points. If the order of the Taylor expansion is fixed for each expansion point, an adaptive algorithm can be used to identify the expansion points. As described in [213], the NDDE formulation is preserved in the reduced model. At each expansion point, the MOR algorithm described in [213] is applied and the corresponding projection matrix $\mathbf{K}_i$, $i = 1, \ldots, n_{\text{points}}$ is computed, where n_{points} denotes the number of expansion points. The final projection matrix $\mathbf{K}$ is based on the orthogonalization of the stack column collection of all single expansion point projection matrices.

Parameterized MOR of both quasi-static and delayed PEEC models have also been proposed in [214], [215], [216], and [217]. Fig. 18 shows the magnitude of the bivariate delayed ROMs of $\mathbf{Y}_{12}(s, L)$ of a power divider, with $L = \{6.4, 8, 9.6\}$ mm) being a geometric parameter [216].

Parameterized reduced order models for sensitivity analysis of PEEC circuits have been presented in [218] and [219].

A different approach is presented in [220] to perform the reduction of quasi-static PEEC models. By introducing a general circuit transformation that can be directly applied to the circuit configuration of the PEEC model, the proposed MOR method progressively reduces the order of the original problem by at least one order of magnitude without involving any matrix operations. Furthermore, another attractive feature of this method is that its computational overhead is dominated by the operation of outer products in combining processes, which takes more than 95% of overall computing time. This feature allows the MOR process to be significantly accelerated by multicore parallel computation using a massive GPU acceleration technology.

X. CONCLUSION

The purpose of this work is to summarize the progress made in PEEC methods over the years. The key uniqueness of the approach is the connection between electromagnetic and circuit theory. This covers the important issue areas of combined systems with integrated circuits and EM problems. Over the course of fifty years, the PEEC method has had many developments and improvements regarding the types of materials that can be treated, the meshers, and the solution methodologies, both in the time and frequency domains. The number of scientific articles dealing with it has steadily increased over time as has the number of applications using it. In particular, its full-wave nature combined with circuit interpretation and rigorous *dc* solution has made it popular with engineers dealing with EMC/SI/PI problems. A lot has been done, the best is yet to come.

REFERENCES

[1] K. S. Yee, "Numerical solution of initial boundary value problems involving Maxwell's equations in isotropic media," *IEEE Trans. Antennas Propag.*, vol. 14, no. 5, pp. 302–307, May 1966.
[2] J. Jin, *The Finite Element Method in Electromagnetics*. Hoboken, NJ, USA: Wiley, 1993.
[3] R. F. Harrington, *Field Computation by Moment Methods*. New York, NY, USA: MacMillan, 1968.
[4] R. F. Harrington, *Field Computation by Moment Methods*. New York, NY, USA: IEEE Press, 1993.
[5] T. Weiland, "A discretization method for the solution of Maxwell's equations for six-component fields," *Electron. Commun. AEU*, vol. 31, no. 3, pp. 116–120, 1977.
[6] A. E. Ruehli, "Inductance calculations in a complex integrated circuit environment," *IBM J. Res. Dev.*, vol. 16, no. 5, pp. 470–481, 1972.
[7] A. Ruehli and P. Brennan, "Efficient capacitance calculations for three-dimensional multiconductor systems," *IEEE Trans. Microw. Theory Techn.*, vol. 21, no. 2, pp. 76–82, Feb. 1973.

[8] A. Ruehli, "Equivalent circuit models for three-dimensional multiconductor systems," *IEEE Trans. Microw. Theory Techn.*, vol. 22, no. 3, pp. 216–221, Mar. 1974.

[9] P. A. Brennan, N. Raver, and A. E. Ruehli, "Three-dimensional inductance computations with partial element equivalent circuits," *IBM J. Res. Dev.*, vol. 23, no. 6, pp. 661–668, 1979.

[10] A. E. Ruehli, "Survey of computer-aided electrical analysis of integrated circuit interconnections," *IBM J. Res. Dev.*, vol. 23, no. 6, pp. 626–639, 1979.

[11] W. Pinello, A. Cangellaris, and A. Ruehli, "Hybrid electromagnetic modeling of noise interactions in packaged electronics based on the partial-element equivalent-circuit formulation," *IEEE Trans. Microw. Theory Techn.*, vol. 45, no. 10, pp. 1889–1896, Oct. 1997.

[12] A. Ruehli and H. Heeb, "Circuit models for three-dimensional geometries including dielectrics," *IEEE Trans. Microw. Theory Techn.*, vol. 40, no. 7, pp. 1507–1516, Jul. 1992.

[13] H. Heeb and A. Ruehli, "Three-dimensional interconnect analysis using partial element equivalent circuits," *IEEE Trans. Circuits Syst. I: Fundam. Theory Appl.*, vol. 39, no. 11, pp. 974–982, Nov. 1992.

[14] G. Antonini, S. Cristina, and A. Orlandi, "PEEC modeling of lightning protection systems and coupling to coaxial cables," *IEEE Trans. Electromagn. Compat.*, vol. 40, no. 4, pp. 481–491, Nov. 1998.

[15] C. Martin, J.-L. Schanen, J.-M. Guichon, and R. Pasterczyk, "Analysis of electromagnetic coupling and current distribution inside a power module," *IEEE Trans. Ind. Appl.*, vol. 43, no. 4, pp. 893–901, Jul./Aug. 2007.

[16] D. Daroui and J. Ekman, "PEEC-based simulations using iterative method and regularization technique for power electronic applications," *IEEE Trans. Electromagn. Compat.*, vol. 56, no. 6, pp. 1448–1456, Dec. 2014.

[17] D. Cottet, I. Stevanović, B. Wunsch, D. Daroui, J. Ekman, and G. Antonini, "Em simulation of planar bus bars in multi-level power converters," in *Proc. Int. Symp. Electromagn. Compat.*, 2012, pp. 1–6.

[18] R. Torchio, F. Lucchini, J.-L. Schanen, O. Chadebec, and G. Meunier, "FFT-PEEC: A fast tool from CAD to power electronics simulations," *IEEE Trans. Power Electron.*, vol. 37, no. 1, pp. 700–713, Jan. 2022.

[19] D. Romano, I. Kovacevic-Badstuebner, G. Antonini, and U. Grossner, "Efficient PEEC iterative solver for power electronic applications," *IEEE Trans. Electromagn. Compat.*, vol. 65, no. 2, pp. 546–554, Apr. 2023.

[20] J. He, P. Zhao, W. Wang, and H. Wang, "Far-field radiation prediction and analysis of a power converter with V-shaped flat cables based on PEEC," *IEEE Trans. Power Electron.*, vol. 38, no. 3, pp. 3246–3256, Mar. 2023.

[21] M. Enohnyaket and J. Ekman, "Analysis of air-core reactors from DC to very high frequencies using PEEC models," *IEEE Trans. Power Del.*, vol. 24, no. 2, pp. 719–729, Apr. 2009.

[22] E. Clavel, J. Roudet, J.-M. Guichon, Z. Gouichiche, P. Joyeux, and A. Derbey, "A nonmeshing approach for modeling grounding," *IEEE Trans. Electromagn. Compat.*, vol. 60, no. 3, pp. 795–802, Jun. 2018.

[23] T. Lindgren, J. Ekman, and S. Backén, "A measurement system for the complex far-field of physically large antenna arrays under noisy conditions utilizing the equivalent electric current method," *IEEE Trans. Antennas Propag.*, vol. 58, no. 10, pp. 3205–3211, Oct. 2010.

[24] P. Scholz, W. Ackermann, T. Weiland, and C. Reinhold, "Antenna modeling for inductive RFID applications using the partial element equivalent circuit method," *IEEE Trans. Magn.*, vol. 46, no. 8, pp. 2967–2970, Aug. 2010.

[25] Y. S. Cao, L. J. Jiang, and A. E. Ruehli, "Distributive radiation and transfer characterization based on the PEEC method," *IEEE Trans. Electromagn. Compat.*, vol. 57, no. 4, pp. 734–742, Aug. 2015.

[26] Y. S. Cao, L. J. Jiang, and A. E. Ruehli, "An equivalent circuit model for graphene-based terahertz antenna using the PEEC method," *IEEE Trans. Antennas Propag.*, vol. 64, no. 4, pp. 1385–1393, Apr. 2016.

[27] C.-C. Chou, W.-C. Lee, and T.-L. Wu, "A rigorous proof on the radiation resistance in generalized PEEC model," *IEEE Trans. Microw. Theory Techn.*, vol. 64, no. 12, pp. 4091–4097, Dec. 2016.

[28] Y. Jiang, Y. Dou, and K.-L. Wu, "Generalized PEEC model for conductor-dielectric problems with radiation effect," *IEEE Trans. Microw. Theory Techn.*, vol. 68, no. 1, pp. 27–38, Jan. 2020.

[29] Y. Dou and K.-L. Wu, "Nature of antenna radiation revealed by physical circuit model," *IEEE Trans. Antennas Propag.*, vol. 69, no. 1, pp. 84–96, Jan. 2021.

[30] Y. Dou and H. Chen, "Method of characteristic modes analysis and manipulation for antenna design by using generalized partial element equivalent circuit," *IEEE J. Multiscale Multiphys. Comput. Tech.*, vol. 8, pp. 123–134, 2023.

[31] J. Wang and K.-L. Wu, "A derived physically expressive circuit model for multilayer RF embedded passives," *IEEE Trans. Microw. Theory Techn.*, vol. 54, no. 5, pp. 1961–1968, May 2006.

[32] J.-T. Kuo, K.-Y. Su, T.-Y. Liu, H.-H. Chen, and S.-J. Chung, "Analytical calculation for DC inductances of rectangular spiral inductors with finite metal thickness in the PEEC formulation," *IEEE Microw. Wireless Compon. Lett.*, vol. 16, no. 2, pp. 69–71, Feb. 2006.

[33] X. Wang et al., "Methodology for analyzing coupling mechanisms in RFI problems based on PEEC," *IEEE Trans. Electromagn. Compat.*, vol. 65, no. 3, pp. 761–769, Jun. 2023.

[34] A. Jazzar, E. Clavel, G. Meunier, B. Vincent, A. Goleanu, and E. Vialardi, "Modeling and simulating the lightning phenomenon: Aeronautic materials comparison in conducted and radiated modes," in *Proc. IEEE Int. Symp. Ind. Electron.*, 2011, pp. 329–334.

[35] E. Clavel, J. Roudet, A.-K. Hayashi Feuerharmel, B. De Luca, Z. Gouichiche, and P. Joyeux, "Benefits of the ground PEEC modeling approach-example of a residential building struck by lightning," *IEEE Trans. Electromagn. Compat.*, vol. 61, no. 6, pp. 1832–1840, Dec. 2019.

[36] I. Hetita, D.-E. A. Mansour, Y. Han, P. Yang, and A. S. Zalhaf, "Experimental and numerical analysis of transient overvoltages of PV systems when struck by lightning," *IEEE Trans. Instrum. Meas.*, vol. 71, 2022, Art. no. 9005611.

[37] I. F. Kovacevic, T. Friedli, A. M. Muesing, and J. W. Kolar, "Full PEEC modeling of EMI filter inductors in the frequency domain," *IEEE Trans. Magn.*, vol. 49, no. 10, pp. 5248–5256, Oct. 2013.

[38] I. F. Kovacevic, T. Friedli, A. M. Muesing, and J. W. Kolar, "3-D electromagnetic modeling of EMI input filters," *IEEE Trans. Ind. Electron.*, vol. 61, no. 1, pp. 231–242, Jan. 2014.

[39] P. Restle, A. Ruehli, S. Walker, and G. Papadopoulos, "Full-wave PEEC time-domain method for the modeling of on-chip interconnects," *IEEE Trans. Comput.-Aided Des. Integr. Circuits Syst.*, vol. 20, no. 7, pp. 877–886, Jul. 2001.

[40] Y. Jiang, W.-J. Zhao, R.X.-K. Gao, E.-X. Liu, and C. E. Png, "A full-wave generalized PEEC model for periodic metallic structure with arbitrary shape," *IEEE Trans. Microw. Theory Techn.*, vol. 70, no. 9, pp. 4110–4119, Sep. 2022.

[41] Z.-X. Wang, P.-C. Zhao, Z.-Y. Zong, W. Wu, and D.-G. Fang, "An extension of partial element equivalent circuit method for frequency selective surface analysis," *IEEE Trans. Antennas Propag.*, vol. 71, no. 1, pp. 1141–1146, Jan. 2023.

[42] Y. Jiang, Y. Dou, and R. X.-K. Gao, "PEEC model based on a novel quasi-static Green's function for two-dimensional periodic structures," *IEEE J. Multiscale Multiphys. Comput. Tech.*, vol. 8, pp. 187–194, 2023.

[43] A. Rosskopf and C. Brunner, "Enhancing Litz wire power loss calculations by combining a sparse strand element equivalent circuit method with a Voronoi-based geometry model," *IEEE Trans. Power Electron.*, vol. 37, no. 9, pp. 11450–11456, Sep. 2022.

[44] J. Lyu, H. Chen, Y. Zhang, Y. Du, and Q. S. Cheng, "Fast simulation of Litz wire using multilevel PEEC method," *IEEE Trans. Power Electron.*, vol. 35, no. 12, pp. 12612–12616, Dec. 2020.

[45] J. Lyu, H. C. Chen, Y. Zhang, Y. Du, and Q. S. Cheng, "Litz wire and uninsulated twisted wire assessment using a multilevel PEEC method," *IEEE Trans. Power Electron.*, vol. 37, no. 2, pp. 2372–2381, Feb. 2022.

[46] J. Lyu, H. C. Chen, Y. Du, and Q. S. Cheng, "Litzimp: A fast impedance extraction algorithm for Litz wire coil," *IEEE Trans. Ind. Electron.*, vol. 70, no. 9, pp. 9326–9335, Sep. 2023.

[47] Y. Li et al., "Modeling and signal integrity analysis of RRAM-based neuromorphic chip crossbar array using partial equivalent element circuit (PEEC) method," *IEEE Trans. Circuits Syst. I: Regular Papers*, vol. 69, no. 9, pp. 3490–3500, Sep. 2022.

[48] G. Gabriadze, G. Chiqovani, A. Demurov, Z. Kutchadze, D. Karkashadze, and R. Jobava, "Fast simulation of PCB/IC/Flex circuit assembly using partial element equivalent circuit method," in *Proc. Int. Symp. Electromagn. Compat.*, 2018, pp. 467–472.

[49] Q. Liu et al., "A SPICE compatible PEEC model with curvilinear RWG basis functions for electromagnetic simulation of lossy flex circuit," in *Proc. IEEE Int. Symp. Antennas Propag. USNC-URSI Radio Sci. Meeting)*, 2022, pp. 1658–1659.

[50] Q. Sun, H. Lv, S. Gao, S. Wang, K. Wei, and M. Mauersberger, "Electromagnetic characteristics analysis of tri-axial HTS cables based on PEEC approach," *IEEE Trans. Appl. Supercond.*, vol. 29, no. 2, Mar. 2019, Art. no. 5400605.

[51] T. Makharashvili et al., "Accurate inductance models of mounted two-terminal decoupling capacitors," *IEEE Trans. Electromagn. Compat.*, vol. 63, no. 1, pp. 237–245, Feb. 2021.

[52] L. Zhu, L. Wang, M. Wu, C. Zhao, and L. Yu, "Precise modeling and design of self-resonant for high-efficiency mid-range wireless power transfer system," *IEEE Trans. Power Electron.*, vol. 38, no. 6, pp. 7848–7862, Jun. 2023.

[53] A. Desmoort et al., "Comparing partial element equivalent circuit and finite element methods for the resonant wireless power transfer 3D modeling," in *Proc. IEEE Conf. Electromagn. Field Computat.*, 2016, pp. 1–1.

[54] R. Li and L. Li, "Partial element equivalent circuit modeling and design for wireless power transfer system via magnetic resonant coupling," *Int. J. Appl. Electromagn. Mech.*, vol. 50, no. 4, pp. 605–615, 2016.

[55] M. Bandinelli et al., "A surface PEEC formulation for high-fidelity analysis of the current return networks in composite aircrafts," *IEEE Trans. Electromagn. Compat.*, vol. 57, no. 5, pp. 1027–1036, Oct. 2015.

[56] J. Nitsch, F. Gronwald, and G. Wollenberg, *Radiating Nonuniform Transmission-Line Systems and the Partial Element Equivalent Circuit Method.* Hoboken, NJ, USA: Wiley, 2009.

[57] A. E. Ruehli, G. Antonini, and L. Jiang, *Circuit Oriented Electromagnetic Modeling Using the PEEC Techniques.* Hoboken, NJ, USA: Wiley, 2017.

[58] Y. Zhu and A. C. Cangellaris, *Multigrid Finite Element Methods for Electromagnetic Field Modeling.* Hoboken, NJ, USA: Wiley, 2006.

[59] R. Araneo, Ed., *Advanced Time Domain Modeling for Electrical Engineering.* London, U.K.: Instit. Eng. Technol., 2022.

[60] A. Ametani, Ed., *Numerical Analysis of Power System Transients and Dynamics.* London, U.K.: Instit. Eng. Technol., 2015.

[61] J. Jayabalan, O. Leong, L. Seng, and M. Iyer, "A scaling technique for partial element equivalent circuit analysis using SPICE," *IEEE Microw. Wireless Compon. Lett.*, vol. 14, no. 5, pp. 216–218, May 2004.

[62] X. Zhang, W. H. Chen, and Z. Feng, "Novel SPICE compatible partial-element equivalent-circuit model for 3-D structures," *IEEE Trans. Microw. Theory Techn.*, vol. 57, no. 11, pp. 2808–2815, Nov. 2009.

[63] C.-C. Chou and T.-L. Wu, "Direct simulation of the full-wave partial element equivalent circuit using standard SPICE [application notes]," *IEEE Microw. Mag.*, vol. 20, no. 6, pp. 22–34, Jun. 2019.

[64] C. Wollenberg and A. Gurisch, "Analysis of 3-D interconnect structures with PEEC using SPICE," *IEEE Trans. Electromagn. Compat.*, vol. 41, no. 4, pp. 412–417, Nov. 1999.

[65] *IEEE Standard for Validation of Computational Electromagnetics Computer Modeling and Simulations*, IEEE Standard 1597, 2008.

[66] C. A. Balanis, *Advanced Engineering Electromagnetics*, 2nd ed. Hoboken, NJ, USA: Wiley, 2012.

[67] J. J. H. Wang, *Generalized Moment Method in Electromagnetics.* Hoboken, NJ, USA: Wiley, 1991.

[68] A. Ruehli, J. Garrett, and C. Paul, "Circuit models for 3D structures with incident fields," in *Proc. Int. Symp. Electromagn. Compat.*, 1993, pp. 28–32.

[69] C.-W. Ho, A. Ruehli, and P. Brennan, "The modified nodal approach to network analysis," *IEEE Trans. Circuits Syst.*, vol. 22, no. 6, pp. 504–509, Jun. 1975.

[70] G. Antonini, M. Di Prinzio, A. Petricola, and A. Ruehli, "Reduced unknowns meshing for the partial element equivalent circuit approach," in *Proc. Int. Symp. Electromagn. Compat.*, 2005, vol. 3, pp. 805–810.

[71] D. Gope, A. Ruehli, C. Yang, and V. Jandhyala, "(S)PEEC: Time- and frequency-domain surface formulation for modeling conductors and dielectrics in combined circuit electromagnetic simulations," *IEEE Trans. Microw. Theory Techn.*, vol. 54, no. 6, pp. 2453–2464, Jun. 2006.

[72] A. E. Ruehli, G. Antonini, and L. J. Jiang, "Skin-effect loss models for time- and frequency-domain PEEC solver," *Proc. IEEE*, vol. 101, no. 2, pp. 451–472, Feb. 2013.

[73] F. D. Murro et al., "Efficient computation of partial elements in the full-wave surface—PEEC method," *IEEE Trans. Electromagn. Compat.*, vol. 63, no. 4, pp. 1189–1201, Aug. 2021.

[74] Y. Wang, D. Gope, V. Jandhyala, and C.-J. Shi, "Generalized Kirchoff's current and voltage law formulation for coupled circuit-electromagnetic simulation with surface integral equations," *IEEE Trans. Microw. Theory Techn.*, vol. 52, no. 7, pp. 1673–1682, Jul. 2004.

[75] S. Chakraborty, "Surface-based broadband electromagnetic-circuit simulation of lossy conductors," *IEE Proc.-Microw., Antennas Propag.*, vol. 153, no. 2, pp. 191–198, Apr. 2006.

[76] K. Coperich, A. Ruehli, and A. Cangellaris, "Enhanced skin effect for partial-element equivalent-circuit (PEEC) models," *IEEE Trans. Microw. Theory Techn.*, vol. 48, no. 9, pp. 1435–1442, Sep. 2000.

[77] L. Daniel, A. Sangiovanni-Vincentelli, and J. White, "Interconnect electromagnetic modeling using conduction modes as global basis functions," in *Proc. IEEE 9th Topical Meeting Elect. Perform. Electron. Packag.*, 2000, pp. 203–206.

[78] L. Daniel, A. Sangiovanni-Vincentelli, and J. White, "Using conduction modes basis functions for efficient electromagnetic analysis of on-chip and off-chip interconnect," in *Proc. 38th Des. Automat. Conf.*, 2001, pp. 563–566.

[79] L. Daniel, A. Sangiovanni-Vincentelli, and J. White, "Proximity templates for modeling of skin and proximity effects on packages and high frequency interconnect," in *Proc. IEEE/ACM Int. Conf. Comput. Aided Des.*, 2002, pp. 326–333.

[80] X. Hu, L. Daniel, and J. White, "Partitioned conduction modes in surface integral equation-based impedance extraction," in *Proc. Elect. Perform. Elect. Packag.*, 2003, pp. 355–358.

[81] A. Ruehli and G. Antonini, "Combined loss mechanism and stability model for the partial element equivalent circuit technique," in *Proc. Appl. Comput. Electromagnetics Conf.*, 2007, pp. 1423–1430.

[82] G. Antonini, A. Orlandi, and A. Ruehli, "Analytical integration of quasi-static potential integrals on nonorthogonal coplanar quadrilaterals for the PEEC method," *IEEE Trans. Electromagn. Compat.*, vol. 44, no. 2, pp. 399–403, May 2002.

[83] A. E. Ruehli, G. Antonini, J. Esch, J. Ekman, A. Mayo, and A. Orlandi, "Nonorthogonal PEEC formulation for time- and frequency-domain EM and circuit modeling," *IEEE Trans. Electromagn. Compat.*, vol. 45, no. 2, pp. 167–176, May 2003.

[84] A. Musing, J. Ekman, and J. W. Kolar, "Efficient calculation of non-orthogonal partial elements for the PEEC method," *IEEE Trans. Magn.*, vol. 45, no. 3, pp. 1140–1143, Mar. 2009.

[85] F. Freschi, G. Gruosso, and M. Repetto, "Unstructured PEEC formulation by dual discretization," *IEEE Microw. Wireless Compon. Lett.*, vol. 16, no. 10, pp. 531–533, Oct. 2006.

[86] F. Freschi and M. Repetto, "A general framework for mixed structured/unstructured PEEC modelling," *Appl. Comput. Electromagn. Soc. J.*, vol. 23, no. 3, pp. 200–206, 2008.

[87] P. Alotto, D. Desideri, F. Freschi, A. Maschio, and M. Repetto, "Dual-PEEC modeling of a two-port TEM cell for VHF applications," *IEEE Trans. Magn.*, vol. 47, no. 5, pp. 1486–1489, May 2011.

[88] J. Siau, G. Meunier, O. Chadebec, J.-M. Guichon, and R. Perrin-Bit, "Volume integral formulation using face elements for electromagnetic problem considering conductors and dielectrics," *IEEE Trans. Electromagn. Compat.*, vol. 58, no. 5, pp. 1587–1594, Oct. 2016.

[89] R. Torchio, P. Alotto, P. Bettini, D. Voltolina, and F. Moro, "A 3-D PEEC formulation based on the cell method for full-wave analyses with conductive, dielectric, and magnetic media," *IEEE Trans. Magn.*, vol. 54, no. 3, Mar. 2018, Art. no. 7201204.

[90] R. Torchio, F. Moro, G. Meunier, J.-M. Guichon, and O. Chadebec, "An extension of unstructured-PEEC method to magnetic media," *IEEE Trans. Magn.*, vol. 55, no. 6, Jun. 2019, Art. no. 7200404.

[91] G. Meunier, J.-M. Guichon, O. Chadebec, B. Bannwarth, L. Krähenbühl, and C. Guérin, "Unstructured-PEEC method for thin electromagnetic media," *IEEE Trans. Magn.*, vol. 56, no. 1, Jan. 2020, Art. no. 7503205.

[92] P. Alotto, F. Freschi, M. Repetto, and C. Rosso, *The Cell Method for Electrical Engineering and Multiphysics Problems: An Introduction.* Berlin, Germany: Springer, 2013.

[93] R. Torchio, "A volume PEEC formulation based on the cell method for electromagnetic problems from low to high frequency," *IEEE Trans. Antennas Propag.*, vol. 67, no. 12, pp. 7452–7465, Dec. 2019.

[94] S. Rao, D. Wilton, and A. Glisson, "Electromagnetic scattering by surfaces of arbitrary shape," *IEEE Trans. Antennas Propag.*, vol. 30, no. 3, pp. 409–418, May 1982.

[95] D. Schaubert, D. Wilton, and A. Glisson, "A tetrahedral modeling method for electromagnetic scattering by arbitrarily shaped inhomogeneous dielectric bodies," *IEEE Trans. Antennas Propag.*, vol. 32, no. 1, pp. 77–85, Jan. 1984.

[96] V. Jandhyala, Y. Wang, D. Gope, and R. Shi, "Coupled electromagnetic-circuit simulation of arbitrarily-shaped conducting structures using triangular meshes," in *Proc. Int. Symp. Qual. Electron. Des.*, 2002, pp. 38–42.

[97] A. Rong, A. Cangellaris, and L. Dong, "Comprehensive broadband electromagnetic modeling of on-chip interconnects with a surface discretization-based generalized PEEC model," *IEEE Trans. Adv. Packag.*, vol. 28, no. 3, pp. 434–444, Aug. 2005.

[98] G. Gabriadze et al., "Enhanced PEEC model based on automatic Voronoi decomposition of triangular meshes," *IEEE Trans. Electromagn. Compat.*, vol. 62, no. 5, pp. 2196–2208, Oct. 2020.

[99] R. Torchio, M. Nolte, S. Schöps, and A. E. Ruehli, "A spline-based partial element equivalent circuit method for electrostatics," *IEEE Trans. Dielectr. Electr. Insul.*, vol. 30, no. 2, pp. 594–601, Apr. 2023.

[100] L. Lombardi, G. Antonini, and A. E. Ruehli, "Analytical evaluation of partial elements using a retarded Taylor series expansion of the Green's function," *IEEE Trans. Microw. Theory Techn.*, vol. 66, no. 5, pp. 2116–2127, May 2018.

[101] M. Štumpf, G. Antonini, and A. Ruehli, "Cagniard–DeHoop technique-based computation of retarded partial coefficients: The coplanar case," *IEEE Access*, vol. 8, pp. 148989–148996, 2020.

[102] M. Štumpf, F. Loreto, G. Pettanice, and G. Antonini, "Cagniard–DeHoop technique-based computation of retarded zero-thickness partial elements," *Eng. Anal. With Boundary Elements*, vol. 137, pp. 56–64, 2022.

[103] M. Štumpf, F. Loreto, G. Pettanice, and G. Antonini, "Partial-inductance retarded partial coefficients: Their exact computation based on the Cagniard–DeHoop technique," *Eng. Anal. With Boundary Elements*, vol. 149, pp. 86–91, 2023.

[104] F. Loreto, D. Romano, M. Stumpf, A. E. Ruehli, and G. Antonini, "Time-domain computation of full-wave partial inductances based on the modified numerical inversion of Laplace transform method," *IEEE Trans. Signal Power Integrity*, vol. 1, pp. 32–42, 2022.

[105] L. Lombardi, D. Romano, and G. Antonini, "Partial element equivalent circuit method modeling of silicon interconnects," *IEEE Trans. Microw. Theory Techn.*, vol. 65, no. 12, pp. 4794–4801, Dec. 2017.

[106] D. Romano and G. Antonini, "Partial element equivalent circuit-based transient analysis of graphene-based interconnects," *IEEE Trans. Electromagn. Compat.*, vol. 58, no. 3, pp. 801–810, Jun. 2016.

[107] Y. S. Cao, P. Li, L. J. Jiang, and A. E. Ruehli, "The derived equivalent circuit model for magnetized anisotropic graphene," *IEEE Trans. Antennas Propag.*, vol. 65, no. 2, pp. 948–953, Feb. 2017.

[108] G. Antonini, A. E. Ruehli, and C. Yang, "PEEC modeling of dispersive and lossy dielectrics," *IEEE Trans. Adv. Packag.*, vol. 31, no. 4, pp. 768–782, Nov. 2008.

[109] A. Hartman, D. Romano, G. Antonini, and J. Ekman, "Partial element equivalent circuit models of three-dimensional geometries including anisotropic dielectrics," *IEEE Trans. Electromagn. Compat.*, vol. 60, no. 3, pp. 696–704, Jun. 2018.

[110] Y. Jiang and K.-L. Wu, "Quasi-static surface-PEEC modeling of electromagnetic problem with finite dielectrics," *IEEE Trans. Microw. Theory Techn.*, vol. 67, no. 2, pp. 565–576, Feb. 2019.

[111] Y. Jiang and R. X.-K. Gao, "Compact quasi-static PEEC modeling of electromagnetic problems with finite-sized dielectrics," *IEEE Trans. Microw. Theory Techn.*, vol. 71, no. 6, pp. 2373–2383, Jun. 2022.

[112] G. Antonini, M. Sabatini, and G. Miscione, "PEEC modeling of linear magnetic materials," in *Proc. IEEE Int. Symp. Electromagn. Compat.*, vol. 1, 2006, pp. 93–98.

[113] D. Romano and G. Antonini, "Quasi-static partial element equivalent circuit models of linear magnetic materials," *IEEE Trans. Magn.*, vol. 51, no. 7, pp. 1–15, Jul. 2015.

[114] N. Xia and Y. Du, "An efficient modeling method for 3-D magnetic plates in magnetic shielding," *IEEE Trans. Electromagn. Compat.*, vol. 56, no. 3, pp. 608–614, Jun. 2014.

[115] D. Romano, G. Antonini, and A. E. Ruehli, "Time-domain partial element equivalent circuit solver including non-linear magnetic materials," *IEEE Trans. Magn.*, vol. 52, no. 9, Sep. 2016, Art. no. 7004911.

[116] A. Astorino, D. Romano, and G. Antonini, "Fast and versatile inverse hysteresis model in quasi-static regime: Derivation and implementation in Simulink and PEEC frameworks," *IEEE Trans. Magn.*, vol. 54, no. 7, Jul. 2018, Art. no. 7300910.

[117] K. Zhao, M. Vouvakis, and J.-F. Lee, "The adaptive cross approximation algorithm for accelerated method of moments computations of EMC problems," *IEEE Trans. Electromagn. Compat.*, vol. 47, no. 4, pp. 763–773, Nov. 2005.

[118] G. Antonini and D. Romano, "Efficient frequency-domain analysis of PEEC circuits through multiscale compressed decomposition," *IEEE Trans. Electromagn. Compat.*, vol. 56, no. 2, pp. 454–465, Apr. 2014.

[119] G. Antonini and D. Romano, "A vectorized multiscale compressed decomposition-based solver for partial element equivalent circuit method," *Int. J. Numer. Modelling: Electron. Netw., Devices Fields*, vol. 28, no. 4, pp. 419–432, 2015.

[120] D. Romano, L. Lombardi, and G. Antonini, "Acceleration of the partial element equivalent circuit method with uniform tessellation-Part I: Identification of geometrical signatures," *Int. J. Numer. Modelling: Electron. Netw., Devices Fields*, vol. 31, no. 6, 2018, Art. no. e2307.

[121] D. Romano, L. Lombardi, and G. Antonini, "Acceleration of the partial element equivalent circuit method with uniform tessellation-Part II: Frequency domain solver with interpolation and reuse of partial elements," *Int. J. Numer. Modelling: Electron. Netw., Devices Fields*, vol. 31, no. 6, 2018, Art. no. e2306.

[122] G. Antonini and A. E. Ruehli, "Fast multipole and multi-function PEEC methods," *IEEE Trans. Mobile Comput.*, vol. 2, no. 4, pp. 288–298, Oct./Dec. 2003.

[123] G. Antonini and D. Romano, "An accurate interpolation strategy for fast frequency sweep of partial element equivalent circuit models," *IEEE Trans. Electromagn. Compat.*, vol. 56, no. 3, pp. 653–658, Jun. 2014.

[124] D. Romano, F. Loreto, G. Antonini, I. Kovacevic-Badstubner, and U. Grossner, "Accelerated partial inductance evaluation via cubic spline interpolation for the PEEC method," in *Proc. 52nd Eur. Microw. Conf.*, 2022, pp. 357–360.

[125] D. Gope, A. E. Ruehli, and V. Jandhyala, "Speeding up PEEC partial inductance computations using a QR-based algorithm," *IEEE Trans. Very Large Scale Integration Syst.*, vol. 15, no. 1, pp. 60–68, Jan. 2007.

[126] A. Polimeridis, J. Villena, L. Daniel, and J. White, "Stable FFT-JVIE solvers for fast analysis of highly inhomogeneous dielectric objects," *J. Comput. Phys.*, vol. 269, pp. 280–296, 2014.

[127] A. C. Yucel, I. P. Georgakis, A. G. Polimeridis, H. Bağcı, and J. K. White, "VoxHenry: FFT-accelerated inductance extraction for voxelized geometries," *IEEE Trans. Microw. Theory Techn.*, vol. 66, no. 4, pp. 1723–1735, Apr. 2018.

[128] M. Wang, C. Qian, J. K. White, and A. C. Yucel, "VoxCap: FFT-accelerated and Tucker-enhanced capacitance extraction simulator for voxelized structures," *IEEE Trans. Microw. Theory Techn.*, vol. 68, no. 12, pp. 5154–5168, Dec. 2020.

[129] M. Wang, C. Qian, E. Di Lorenzo, L. J. Gomez, V. Okhmatovski, and A. C. Yucel, "SuperVoxHenry: Tucker-enhanced and FFT-accelerated inductance extraction for voxelized superconducting structures," *IEEE Trans. Appl. Supercond.*, vol. 31, no. 7, Oct. 2021, Art. no. 1101911.

[130] W. Hackbusch, "A sparse matrix arithmetic based on H-matrices. Part I: Introduction to H-matrices," *Computing*, vol. 62, no. 2, pp. 89–108, Apr. 1999.

[131] R. Torchio, P. Bettini, and P. Alotto, "PEEC-based analysis of complex fusion magnets during fast voltage transients with h-matrix compression," *IEEE Trans. Magn.*, vol. 53, no. 6, Jun. 2017, Art no. 7200904.

[132] R. Torchio, L. Codecasa, L. Di Rienzo, and F. Moro, "Fast uncertainty quantification in low frequency electromagnetic problems by an integral equation method based on hierarchical matrix compression," *IEEE Access*, vol. 7, pp. 163919–163932, 2019.

[133] D. Romano, G. Antonini, M. D'Emidio, D. Frigioni, A. Mori, and M. Bandinelli, "Rigorous *dc* solution of partial element equivalent circuit models," *IEEE Trans. Circuits Syst. I: Regular Papers*, vol. 63, no. 9, pp. 1499–1510, Sep. 2016.

[134] D. Romano, I. Kovacevic-Badstubner, M. Parise, U. Grossner, J. Ekman, and G. Antonini, "Rigorous *dc* solution of partial element equivalent circuit models including conductive, dielectric, and magnetic materials," *IEEE Trans. Electromagn. Compat.*, vol. 62, no. 3, pp. 870–879, Jun. 2020.

[135] S. V. Kochetov, M. Leone, and G. Wollenberg, "PEEC formulation based on dyadic Green's functions for layered media in the time and frequency domains," *IEEE Trans. Electromagn. Compat.*, vol. 50, no. 4, pp. 953–965, Nov. 2008.

[136] Z.-Y. Zong, W. Wu, F. Ling, J. Chen, and D.-G. Fang, "Efficient low-frequency breakdown free full-wave PEEC modeling based on geometrical optics DCIM," *IEEE Trans. Microw. Theory Techn.*, vol. 60, no. 6, pp. 1500–1512, Jun. 2012.

[137] H. Wang and J. Fan, "Modeling local via structures using innovative PEEC formulation based on cavity Green's functions with wave port excitation," *IEEE Trans. Microw. Theory Techn.*, vol. 61, no. 5, pp. 1748–1757, May 2013.

[138] X. Sun, T. Huang, L. Ye, Y. Sun, S. Jin, and J. Fan, "Analyzing multiple vias in a parallel-plate pair based on a nonorthogonal PEEC method," *IEEE Trans. Electromagn. Compat.*, vol. 61, no. 5, pp. 1602–1611, Oct. 2019.

[139] L. Ye et al., "Modeling stripline with slotted ground plane in multilayered circuit board using PEEC formulation," *IEEE Trans. Electromagn. Compat.*, vol. 62, no. 1, pp. 280–284, Feb. 2020.

[140] C. Li, B. Zhao, B. Pu, X. Wang, D. Kim, and J. Fan, "PEEC-based on-chip PDN impedance modeling using layered Green's function," in *Proc. IEEE Int. Symp. Electromagn. Compat. Signal/Power Integrity*, 2022, pp. 164–168.

[141] B. Zhao et al., "Physics-based circuit modeling methodology for system power integrity analysis and design," *IEEE Trans. Electromagn. Compat.*, vol. 62, no. 4, pp. 1266–1277, Aug. 2020.

[142] B. Zhao, S. Bai, J. Fan, B. Achkir, and A. Ruehli, "PEEC modeling in 3D IC/Packaging applications based on layered Green's functions," *IEEE Trans. Signal Power Integrity*, vol. 2, pp. 23–31, 2023.

[143] P. Yutthagowith, A. Ametani, N. Nagaoka, and Y. Baba, "Application of the partial element equivalent circuit method to analysis of transient potential rises in grounding systems," *IEEE Trans. Electromagn. Compat.*, vol. 53, no. 3, pp. 726–736, Aug. 2011.

[144] Y. Du, X. Wang, and M. Chen, "Circuit parameters of vertical wires above a lossy ground in PEEC models," *IEEE Trans. Electromagn. Compat.*, vol. 54, no. 4, pp. 871–879, Aug. 2012.

[145] H. Chen, Y. Du, and M. Chen, "Lightning transient analysis of radio base stations," *IEEE Trans. Power Del.*, vol. 33, no. 5, pp. 2187–2197, Oct. 2018.

[146] H. Chen, Y. Zhang, Y. Du, and Q. S. Cheng, "Lightning propagation analysis on telecommunication towers above the perfect ground using full-wave time domain PEEC method," *IEEE Trans. Electromagn. Compat.*, vol. 61, no. 3, pp. 697–704, Jun. 2019.

[147] R. Qi, Y. Du, and M. Chen, "Lightning-generated transients in buildings with an efficient PEEC method," *IEEE Trans. Magn.*, vol. 55, no. 11, Nov. 2019, Art. no. 7502605.

[148] R. Qi, Y. P. Du, and M. Chen, "Time-domain PEEC transient analysis for a wire structure above the perfectly conducting ground with the incident field from a distant lightning channel," *IEEE Trans. Electromagn. Compat.*, vol. 62, no. 5, pp. 1787–1795, Oct. 2020.

[149] Y. Zhang, H. Chen, Y. Du, Z. Li, and Y. Wu, "Lightning transient analysis of main and submain circuits in commercial buildings using PEEC method," *IEEE Trans. Ind. Appl.*, vol. 56, no. 1, pp. 106–116, Jan./Feb. 2020.

[150] R. Qi, Y. Ding, Y. P. Du, M. Chen, and Z. Li, "Evaluation of Green's functions for PEEC models in the air and lossy-ground space," *IEEE Trans. Electromagn. Compat.*, vol. 63, no. 6, pp. 1930–1940, Dec. 2021.

[151] J. Jia, L. Shi, and J. Si, "Modeling large-size round steel plates with surface PEEC method for lightning transient analysis," *IEEE Trans. Electromagn. Compat.*, vol. 64, no. 3, pp. 805–815, Jun. 2022.

[152] W. Ye, W. Liu, N. Xiang, K. Li, and W. Chen, "A full-wave PEEC model for thin-wire structure in the air and homogeneous lossy ground," *IEEE Trans. Electromagn. Compat.*, vol. 65, no. 2, pp. 518–527, Apr. 2023.

[153] R. Torchio et al., "A reduced order modelling approach for full-Maxwell lightning strike analyses in layered backgrounds," *IEEE Trans. Power Del.*, vol. 38, no. 3, pp. 1949–1957, Jun. 2023.

[154] C. Gianfagna, L. Lombardi, and G. Antonini, "Marching-on-in-time solution of delayed PEEC models of conductive and dielectric objects," *IET Microw., Antennas Propag.*, vol. 13, no. 1, pp. 42–47, 2019.

[155] L. Lombardi, R. Raimondo, and G. Antonini, "Electrothermal formulation of the partial element equivalent circuit method," *Int. J. Numer. Modelling: Electron. Netw., Devices Fields*, vol. 31, no. 4, 2018, Art. no. e2253.

[156] G. Antonini and A. E. Ruehli, "Waveform relaxation time domain solver for subsystem arrays," *IEEE Trans. Adv. Packag.*, vol. 33, no. 4, pp. 760–768, Nov. 2010.

[157] L. Lombardi, P. Belforte, and G. Antonini, "Digital wave simulation of quasi-static partial element equivalent circuit method," *IEEE Trans. Electromagn. Compat.*, vol. 59, no. 2, pp. 429–438, Apr. 2017.

[158] J. Park, J. Lee, B. Seol, and J. Kim, "Efficient calculation of inductive and capacitive coupling due to electrostatic discharge (ESD) using PEEC method," *IEEE Trans. Electromagn. Compat.*, vol. 57, no. 4, pp. 743–753, Aug. 2015.

[159] J. Park, J. Lee, B. Seol, and J. Kim, "Fast and accurate calculation of system-level ESD noise coupling to a signal trace by PEEC model decomposition," *IEEE Trans. Microw. Theory Techn.*, vol. 65, no. 1, pp. 50–61, Jan. 2017.

[160] J. Lambert, *Numerical Methods for Ordinary Differential Systems: The Initial Value Problem*. Hoboken, NJ, USA: Wiley, 1991.

[161] A. Ruehli, U. Miekkala, and H. Heeb, "Stability of discretized partial element equivalent EFIE circuit models," *IEEE Trans. Antennas Propag.*, vol. 43, no. 6, pp. 553–559, Jun. 1995.

[162] J. Garrett, A. Ruehli, and C. Paul, "Accuracy and stability improvements of integral equation models using the partial element equivalent circuit (PEEC) approach," *IEEE Trans. Antennas Propag.*, vol. 46, no. 12, pp. 1824–1832, Dec. 1998.

[163] S. Kochetov and G. Wollenberg, "Stability of full-wave PEEC models: Reason for instabilities and approach for correction," *IEEE Trans. Electromagn. Compat.*, vol. 47, no. 4, pp. 738–748, Nov. 2005.

[164] S. Kochetov and G. Wollenberg, "Stable time domain solution of EFIE via full-wave PEEC modeling," in *Proc. 6th Int. Symp. Electromagn. Compat. Electromagn. Ecol.*, 2005, pp. 54–57.

[165] S. Kochetov and G. Wollenberg, "Stable time domain PEEC solution for pulse interconnection structures," in *Proc. Int. Symp. Electromagn. Compat.*, vol. 3, 2005, pp. 911–916.

[166] S. V. Kochetov and G. Wollenberg, "Stable and effective full-wave PEEC models by full-spectrum convolution macromodeling," *IEEE Trans. Electromagn. Compat.*, vol. 49, no. 1, pp. 25–34, Feb. 2007.

[167] A. Bellen, N. Guglielmi, and A. Ruehli, "Methods for linear systems of circuit delay differential equations of neutral type," *IEEE Trans. Circuits Syst. I: Fundam. Theory Appl.*, vol. 46, no. 1, pp. 212–215, Jan. 1999.

[168] D. Yue and Q.-L. Han, "A delay-dependent stability criterion of neutral systems and its application to a partial element equivalent circuit model," *IEEE Trans. Circuits Syst. II: Exp. Briefs*, vol. 51, no. 12, pp. 685–689, 2004.

[169] G. Antonini and P. Pepe, "Input-to-state stability analysis of partial-element equivalent-circuit models," *IEEE Trans. Circuits Syst. I: Regular Papers*, vol. 56, no. 3, pp. 673–684, Mar. 2009.

[170] X.-M. Zhang and Q.-L. Han, "A new stability criterion for a partial element equivalent circuit model of neutral type," *IEEE Trans. Circuits Syst. II: Exp. Briefs*, vol. 56, no. 10, pp. 798–802, Oct. 2009.

[171] C.-C. Chou and T.-L. Wu, "Poles and stability of full-wave PEEC," *IEEE Trans. Antennas Propag.*, vol. 69, no. 2, pp. 950–961, Feb. 2021.

[172] A. Ruehli, U. Miekkala, A. Bellen, and H. Heeb, "Stable time domain solutions for EMC problems using PEEC circuit models," in *Proc. IEEE Symp. Electromagn. Compat.*, 1994, pp. 371–376.

[173] R. Griffith and M. S. Nakhla, "Mixed frequency/time domain analysis of nonlinear circuits," *IEEE Trans. Comput.-Aided Des. Integr. Circuits Syst.*, vol. 11, no. 8, pp. 1032–1043, Aug. 1992.

[174] M. Nakhla, K. Singhal, and J. Vlach, "Numerical inversion of the Laplace transform," *Electron. Lett.*, vol. 9, no. 14, pp. 313–314, 1973.

[175] W. R. LePage, *Complex Variables and the Laplace Transform for Engineers*. New York, NY, USA: Dover Publications, Inc., 1961.

[176] G. A. Baker and P. Graves-Morris, *Padé Approximants: Encyclopedia of Mathematics*. New York, NY, USA: Cambridge Univ. Press, 1995, .

[177] J. Vlach and K. Singhal, *Computer Methods for Circuit Analysis and Design*, 2nd ed. Boston, MA, USA: Kluwer Academic, 2003.

[178] Y. Tao, E. Gad, and M. Nakhla, "Fast and stable time-domain simulation based on modified numerical inversion of the laplace transform," *IEEE Trans. Compon. Packag. Manuf. Technol.*, vol. 11, no. 5, pp. 848–858, May 2021.

[179] L. Lombardi et al., "Time-domain analysis of retarded partial element equivalent circuit models using numerical inversion of Laplace transform," *IEEE Trans. Electromagn. Compat.*, vol. 63, no. 3, pp. 870–879, Jun. 2021.

[180] F. Loreto et al., "Modified numerical inversion of laplace transform methods for the time-domain analysis of retarded partial elements equivalent circuit models," *IEEE Trans. Electromagn. Compat.*, vol. 64, no. 6, pp. 2179–2188, Dec. 2022.

[181] Z. Chen and M. M. Ney, "The method of weighted residuals: A general approach to deriving time- and frequency-domain numerical methods," *IEEE Antennas Propag. Mag.*, vol. 51, no. 1, pp. 51–70, Feb. 2009.

[182] Z. Chen, C.-F. Wang, and W. J. R. Hoefer, "A unified view of computational electromagnetics," *IEEE Trans. Microw. Theory Techn.*, vol. 70, no. 2, pp. 955–969, Feb. 2022.

[183] J. S. Zhao and W. C. Chew, "Integral equation solution of Maxwell's equation from zero frequency to microwave frequencies," *IEEE Trans. Antennas Propag.*, vol. 48, pp. 1635–1645, Oct. 2000.

[184] Z.-G. Qian and W. C. Chew, "Enhanced A-EFIE with perturbation method," *IEEE Trans. Antennas Propag.*, vol. 58, no. 10, pp. 3256–3264, Oct. 2010.

[185] T. Xia et al., "An enhanced augmented electric-field integral equation formulation for dielectric objects," *IEEE Trans. Antennas Propag.*, vol. 64, no. 6, pp. 2339–2347, Jun. 2016.

[186] D. Gope, A. Ruehli, and V. Jandhyala, "Solving low-frequency EM-CKT problems using the PEEC method," *IEEE Trans. Adv. Packag.*, vol. 30, no. 2, pp. 313–320, May 2007.

[187] L. Grasedyck and W. Hackbusch, "Construction and arithmetics of H-matrices," *Computing*, vol. 70, no. 4, pp. 295–334, Apr. 2003.

[188] M. Bebendorf, *Hierarchical Matrices: A Means to Efficiently Solve Elliptic Boundary Value Problems*, 1st ed. Berlin, Germany: Springer, 2008.

[189] G. Antonini and D. Romano, "Adaptive-cross-approximation-based acceleration of transient analysis of quasi-static partial element equivalent circuits," *IET Microw., Antennas Propag.*, vol. 9, no. 9, pp. 700–70, May 2015.

[190] A. Heldring, J. M. Tamayo, E. Ubeda, and J. M. Rius, "Accelerated direct solution of the method-of-moments linear system," *Proc. IEEE*, vol. 101, no. 2, pp. 364–371, Feb. 2013.

[191] D. Voltolina, P. Bettini, P. Alotto, F. Moro, and R. Torchio, "High-performance PEEC analysis of electromagnetic scatterers," *IEEE Trans. Magn.*, vol. 55, no. 6, Jun. 2019, Art. no. 7201204.

[192] D. Voltolina, R. Torchio, P. Bettini, R. Cavazzana, and M. Moresco, "PEEC modeling of planar spiral resonators," *IEEE Trans. Magn.*, vol. 56, no. 1, 2020, Art. no. 6700404.

[193] L. Greengard and V. Rokhlin, "A fast algorithm for particle simulations," *J. Comput. Phys.*, vol. 73, no. 2, pp. 325–348, 1987.

[194] J. Barnes and A. Hut, "Hierarchical $O(n \log n)$ force-calculation algorithm," *Nature*, vol. 324, no. 6096, pp. 446–449, 1986.

[195] T. A. Davis and I. S. Duff, "An unsymmetric-pattern multifrontal method for sparse LU factorization," *SIAM J. Matrix Anal. Appl.*, vol. 18, no. 1, pp. 140–158, Jan. 1997.

[196] I. S. Duff and J. Koster, "The design and use of algorithms for permuting large entries to the diagonal of sparse matrices," *SIAM J. Matrix Anal. Appl.*, vol. 20, no. 4, pp. 889–901, 1999.

[197] I. S. Duff and J. Koster, "On algorithms for permuting large entries to the diagonal of a sparse matrix," *SIAM J. Matrix Anal. Appl.*, vol. 22, no. 4, pp. 973–996, 2001.

[198] G. Pettanice, F. Loreto, R. Valentini, P. Di Marco, and G. Antonini, "Time domain analysis of PEEC models through the FFT acceleration technique," in *Proc. 17th Eur. Conf. Antennas Propag.*, 2023, pp. 1–5.

[199] S. X.-D. Tan and L. He, *Advanced Model Order Reduction Techniques in VLSI Design*. Cambridge, U.K.: C. U. Press, 2007.

[200] P. Benner et al. Eds., *System- and Data-Driven Methods and Algorithms*, vol. 1, Berlin, Germany: De Gruyter, 2021.

[201] R. Slone, W. Smith, and Z. Bai, "Using partial element equivalent circuit full wave analysis and Pade via Lanczos to numerically simulate EMC problems," in *Proc. IEEE EMC Austine Style IEEE 1997 Int. Symp. Electromagn. Compat. Symp. Rec.*, 1997, pp. 608–613.

[202] N. Marques, M. Kamon, J. White, and L. Silveira, "An efficient algorithm for fast parasitic extraction and passive order reduction of 3d interconnect models," in *Proc. Des., Automat. Test Europe*, 1998, pp. 538–543.

[203] N. Marques, M. Kamon, J. White, and L. Silveira, "A mixed nodal-mesh formulation for efficient extraction and passive reduced-order modeling of 3D interconnects," in *Proc. 35th Des. Automat. Conf.*, 1998, pp. 297–302.

[204] H. Heeb, A. Ruehli, J. Bracken, and R. Rohrer, "Three dimensional circuit oriented electromagnetic modeling for vlsi interconnects," in *Proc. IEEE Int. Conf. Comput. Design: VLSI Comput. Processors*, 1992, pp. 218–221.

[205] E. Chiprout, H. Heeb, M. Nakhla, and A. Ruehli, "Simulating 3-D retarded interconnect models using complex frequency hopping (CFH)," in *Proc. Int. Conf. Comput. Aided Des.*, 1993, pp. 66–72.

[206] E. Chiprout and M. Nakhla, *Asymptotic Waveform Evaluation*. Boston, MA, USA: KLUWER, 1994.

[207] J. Phillips, E. Chiprout, and D. Ling, "Efficient full-wave electromagnetic analysis via model-order reduction of fast integral transforms," in *Proc. 33rd Des. Automat. Conf. Proc.*, 1996, pp. 377–382.

[208] A. Odabasioglu, M. Celik, and L. Pileggi, "PRIMA: Passive reduced-order interconnect macromodeling algorithm," *IEEE Trans. Comput.-Aided Des. Integr. Circuits Syst.*, vol. 17, no. 8, pp. 645–654, Aug. 1998.

[209] R. W. Freund, "Krylov-subspace methods for reduced-order modeling in circuit simulation," *J. Comput. Appl. Math.*, vol. 123, pp. 395–421, 2000.

[210] J. Cullum, A. Ruehli, and T. Zhang, "A method for reduced-order modeling and simulation of large interconnect circuits and its application to PEEC models with retardation," *IEEE Trans. Circuits Syst. II: Analog Digit. Signal Process.*, vol. 47, no. 4, pp. 261–273, Apr. 2000.

[211] Elfadel and Ling, "A block rational Arnoldi algorithm for multipoint passive model-order reduction of multiport RLC networks," in *Proc. IEEE Int. Conf. Comput. Aided Des.*, 1997, pp. 66–71.

[212] F. Ferranti, M. S. Nakhla, G. Antonini, T. Dhaene, L. Knockaert, and A. E. Ruehli, "Multipoint full-wave model order reduction for delayed PEEC models with large delays," *IEEE Trans. Electromagn. Compat.*, vol. 53, no. 4, pp. 959–967, Nov. 2011.

[213] W. Tseng, C. Chen, E. Gad, M. Nakhla, and R. Achar, "Passive order reduction for RLC circuits with delay elements," *IEEE Trans. Adv. Packag.*, vol. 30, no. 4, pp. 830–840, Nov. 2007.

[214] F. Ferranti, G. Antonini, T. Dhaene, and L. Knockaert, "Guaranteed passive parameterized model order reduction of the partial element equivalent circuit (PEEC) method," *IEEE Trans. Electromagn. Compat.*, vol. 52, no. 4, pp. 974–984, Nov. 2010.

[215] F. Ferranti, G. Antonini, T. Dhaene, L. Knockaert, and A. E. Ruehli, "Physics-based passivity-preserving parameterized model order reduction for PEEC circuit analysis," *IEEE Trans. Compon. Packag. Manuf. Technol.*, vol. 1, no. 3, pp. 399–409, Mar. 2011.

[216] F. Ferranti, M. Nakhla, G. Antonini, T. Dhaene, L. Knockaert, and A. E. Ruehli, "Interpolation-based parameterized model order reduction of delayed systems," *IEEE Trans. Microw. Theory Techn.*, vol. 60, no. 3, pp. 431–440, Mar. 2012.

[217] L. Lombardi, Y. Tao, B. Nouri, F. Ferranti, G. Antonini, and M. S. Nakhla, "Parameterized model order reduction of delayed PEEC circuits," *IEEE Trans. Electromagn. Compat.*, vol. 62, no. 3, pp. 859–869, Jun. 2020.

[218] L. De Camillis, F. Ferranti, G. Antonini, D. Vande Ginste, and D. De Zutter, "Parameterized partial element equivalent circuit method for sensitivity analysis of multiport systems," *IEEE Trans. Compon. Packag. Manuf. Technol.*, vol. 2, no. 2, pp. 248–255, Feb. 2012.

[219] L. De Camillis, F. Ferranti, and G. Antonini, "Parameterized model order reduction for efficient time and frequency domain global sensitivity analysis of PEEC circuits," *ACES J.*, vol. 31, no. 10, pp. 1170–1180, 2016.

[220] Y. Dou and K.-L. Wu, "Direct mesh-based model order reduction of PEEC model for quasi-static circuit problems," *IEEE Trans. Microw. Theory Techn.*, vol. 64, no. 8, pp. 2409–2422, Aug. 2016.

Giulio Antonini (Senior Member, IEEE) received the laurea degree (Hons.) in electrical engineering from the University of L'Aquila, L'Aquila, Italy, in 1994, and the Ph.D. degree in electrical engineering from the University of Rome "La Sapienza," Rome, Italy, in 1998.

Since 1998, he has been with the UAq EMC Laboratory, University of L'Aquila, where he is currently a Professor. He has authored more than 300 papers published in international journals and in the proceedings of international conferences. He has coauthored the book "*Circuit Oriented Electromagnetic Modeling Using the PEEC Techniques*," (Wiley–IEEE Press, 2017). His research interest includes computational electromagnetics.

Albert E. Ruehli (Life Fellow, IEEE) received the Ph.D. degree in electrical engineering from the University of Vermont, Burlington, VT, USA, in 1972, and an honorary Doctorate degree from Lulea University, Lulea, Sweden, in 2007.

He has been a member of various projects with IBM including interconnect tools and modeling and Manager of both a VLSI design and CAD group. From 1972 to 2009, he was with IBM's T.J. Watson Research Center, Yorktown Heights, NY, USA. He is currently an Adjunct Professor with the Missouri University of S&T, Rolla, MO, USA. He has edited two books and authored/coauthoredanother book and over 250 technical papers.

Dr. Ruehli is a Member of Society for Industrial and Applied Mathematics. He was the recipient of five IBM Awards, the Guillemin-Cauer Prize in 1982, and the Golden Jubilee Medal from the IEEE Circuits and Systems Society in 1999. He was also the recipient of a Certificate of Achievement from the IEEE Electromagnetic Compatibility (EMC) Society in 2001, the 2005 Richard R Stoddart Award, and the Honorary Life Member Award from the IEEE EMC Society in 2007.

Daniele Romano was born in Campobasso, Italy, in 1984. He received the laurea degree in computer science and automation engineering and the Ph.D. degree in industrial engineering from the University of L'Aquila, L'Aquila, Italy, in 2012 and 2018, respectively.

Since 2012, he has been with the UAq EMC Laboratory, University of L'Aquila, where he is currently a Researcher. His research interests include EMC modeling and analysis, algorithm engineering, and speed-up techniques applied to EMC problems.

Fabrizio Loreto was born in L'Aquila, Italy, in 1993. He received the master's degree (Hons.) in electrical engineering, in 2020, from the University of L'Aquila, L'Aquila, Italy, where he is currently working toward the Ph.D. degree in industrial and information engineering.

His research interests include time-domain modeling for EMC-EMI problems with emphasis on the partial element equivalent circuit method.